Accepted Manuscript

Multifunctional thioxanthone derivatives with acetylcholinesterase, monoamine oxidases and β-amyloid aggregation inhibitory activities as potential agents against Alzheimer's disease

Li Luo, Yan Li, Xiaoming Qiang, Zhongcheng Cao, Rui Xu, Xia Yang, Ganyuan Xiao, Qing Song, Zhenghuai Tan, Yong Deng

PII: S0968-0896(17)30050-0
DOI: http://dx.doi.org/10.1016/j.bmc.2017.02.027
Reference: BMC 13556

To appear in: *Bioorganic & Medicinal Chemistry*

Received Date: 11 January 2017
Revised Date: 10 February 2017
Accepted Date: 12 February 2017

Please cite this article as: Luo, L., Li, Y., Qiang, X., Cao, Z., Xu, R., Yang, X., Xiao, G., Song, Q., Tan, Z., Deng, Y., Multifunctional thioxanthone derivatives with acetylcholinesterase, monoamine oxidases and β-amyloid aggregation inhibitory activities as potential agents against Alzheimer's disease, *Bioorganic & Medicinal Chemistry* (2017), doi: http://dx.doi.org/10.1016/j.bmc.2017.02.027

Multifunctional thioxanthone derivatives with acetylcholinesterase, monoamine oxidases and *β*-amyloid aggregation inhibitory activities as potential agents against Alzheimer's disease

Li Luo[a,#], Yan Li[a,#], Xiaoming Qiang[a], Zhongcheng Cao[a], Rui Xu[a], Xia Yang[a], Ganyuan Xiao[a], Qing Song[a], Zhenghuai Tan[b,*], Yong Deng[a,*]

[a]*Department of Medicinal Chemistry, Key Laboratory of Drug Targeting and Drug Delivery System of the Education Ministry, West China School of Pharmacy, Sichuan University, Chengdu, 610041, China*

[b]*Institute of Traditional Chinese Medicine Pharmacology and Toxicology, Sichuan academy of Chinese Medicine Sciences, Chengdu, 610041, China*

# These authors contributed equally to this work.

**Corresponding Author*.

Phone, +86-28-85258982; E-mail: tanzhh616@163.com (Zhenghuai Tan)

Phone, +86-28-85503790; E-mail: dengyong@scu.edu.cn (Yong Deng)

Abstract

A series of 1-hydroxyl-3-aminoalkoxy-thioxanthone derivatives were designed, synthesized and evaluated as potential multifunctional agents against Alzheimer's disease (AD). The results indicated that most of these compounds exhibited good AChE and MAOs inhibitory activities, significant inhibition of self- and Cu^{2+}-induced A$\beta_{1\text{-}42}$ aggregation, and moderate to good antioxidant activities. Specifically, compound **9e** displayed high inhibitory potency toward AChE (IC_{50} = 0.59 ± 0.02 μM), MAO-A and MAO-B (IC_{50} = 1.01 ± 0.02 μM and 0.90 ± 0.01 μM respectively), excellent efficiency to block both self- and Cu^{2+}-induced A$\beta_{1\text{-}42}$ aggregation (74.8 ± 1.2% and 87.7 ± 1.9% at 25 μM, respectively), good metal-chelating property and a low toxicity in SH-SY5Y cells. Furthermore, kinetic and molecular modeling studies revealed that compound **9e** binds simultaneously to the catalytic active site and peripheral anionic site of AChE, and could penetrate the BBB. Collectively, these results suggested that **9e** might be a potential multifunctional agent for further development in the treatment of AD.

Keywords: Alzheimer's disease; thioxanthone derivatives; multifunctional agents; acetylcholinesterase inhibitors; anti-Aβ aggregation; monoamine oxidase inhibitors.

1. Introduction

Alzheimer's disease (AD) is a multifaceted and progressive neurodegenerative disorder characterized by memory loss, severe behavioral abnormalities, cognitive impairment and ultimately death. And it is the most common manifestation of dementia in the elderly population.[1] Although the etiology of AD is not completely known, several factors have been considered to play significant roles in the pathogenesis, including the development of deposits of β-amyloid (Aβ) and τ-protein, dyshomeostasis of biometals, oxidative stress and deficit of acetylcholine (ACh). Several hypotheses based on these factors have been proposed to explain the mechanism of AD development.[2,3]

Acetylcholinesterase (AChE) and butyrylcholinesterase (BuChE) are the two major forms of cholinesterases in brain, and the AChE has attracted more attention since it could hydrolyze the majority of ACh.[4] According to the cholinergic hypothesis, the cognitive and memory deterioration of AD is due to the deficit of ACh in specific regions of the brain.[5] Currently, AChE inhibitors are the most effective drugs for the treatment of AD.[6] In addition, studies showed that AChE facilitates amyloid fibril formation, obtaining stable AChE-Aβ complexes, which are more toxic than single Aβ peptide.[7] Dual-site inhibitors, which interact with both the catalytic active site (CAS) and peripheral anionic site (PAS) of AChE can not only stimulate the cholinergic system, but also inhibit the AChE-promoted Aβ production and aggregation.[8] Thus, AChE is an important therapeutic target for the treatment of AD.

Amyloid hypothesis, the most predominant hypothesis, asserts that an increased production and accumulation of Aβ peptide in the brain was considered to initiate the pathogenic cascade, ultimately lead to neuronal loss and dementia.[9] A$\beta_{1\text{-}40}$ and A$\beta_{1\text{-}42}$ are the primary isoforms of Aβ peptides. A$\beta_{1\text{-}42}$ displays a higher neuronal toxicity and aggregates more quickly than A$\beta_{1\text{-}40}$, though the amount of former is only 10% of the latter.[10] Therefore, impeding the formation and deposition of A$\beta_{1\text{-}42}$ is thought to be a pivotal strategy for AD treatment.

Monoamine oxidase A and B (MAO-A and -B) are flavin adenine dinucleotide (FAD)-containing enzymes, which show different substrate specificity and sensitivity to inhibitors.[11] As known, most of the AD patients suffer from psychological symptoms such as depression and psychosis. MAO-A inhibitors are used as antidepressants such as toloxatone and moclobemide, and selective MAO-B inhibitors, such as rasagiline and selegiline, are beneficial for the treatment of neurodegenerative disorders like AD.[12] Besides, the biochemical activity of MAOs generates

hydrogen peroxide and gives rise to oxidative stress.[12,13] Hence, MAOs are important factors that involoved in AD pathogenesis.

Recently, studies has demonstrated that oxidative stress is a central event in initiating the Aβ aggregation and τ-protein hyperphosphorylation, involved in the early stage of the pathologic cascade.[14,15] Consequently, drugs that specifically scavenge oxygen radicals might be useful for the prevention or treatment of AD. In addition, there is increasing evidence that elevated concentrations of the metal ions such as Cu^{2+}, Zn^{2+}, Fe^{2+} and Al^{3+} clearly exists in AD brains.[16] The high levels of these redox-active metals could promote the generation of reactive oxygen species (ROS) and oxidative stress.[17,18] Additionally, the abnormal accumulation of these metal ions is able to accelerate the formation of Aβ plaques and neurofibrillary tangles (NFT), which could cause inflammation and neurotoxicity.[18,19] Accordingly, modulation of such biometals in brain has become a promising therapeutic strategy for interdicting AD pathogenesis.

Due to the multifactorial pathogenesis of AD as mentioned above, the "multitarget-directed ligands" (MTDLs) strategy seems more efficient. Compared to single-targeted drugs, it believes that compounds with two or more distinct pharmacological properties closely related to the neurodegenerative process are more effective in AD therapy.[20-22]

To date, it was reported that natural xanthones and their derivatives could inhibit both AChE and BuChE, self-induced Aβ aggregation and serve as potential antioxidants and biometal chelators.[23-25] Thioxanthone (**I**, **Figure 1**, 9*H*-thioxanthen-9-one), a bioisostere of xanthone (**II**, **Figure 1**), is the core structure of various natural occurring and synthetic compounds that exhibits broad pharmacological activities such as anticancer[26], antiparasitic[27] and MAO-A inhibitory activities.[28] However, there are no reports about the research on thioxanthone derivates against AD. Considering sulfur atom, as the isostere of oxygen in xanthone nucleus, is easier to lose electron and can allows thioxanthones to display higher antioxidant potency. Furthermore, thioxanthones have better lipid solubility and permeability. Therefore, thioxanthone could be used as a promising lead compound in the design of multifunctional agents against AD. Recently, our group has reported a 7,4′-*O*-modified genistein derivative (**III**) as the potential multifunctional agent for AD treatment, and described the benzylamine moieties as AChE inhibitory pharmacophores.[29] However, this compound showed low inhibitory effect on self-induced A$\beta_{1\text{-}42}$ aggregation. Therefore, according to the MTDLs strategy, we combined 1,3-dihydroxy-9*H*-thioxanthen-9-one (**IV**) with appropriate

secondary amines using different lengths of carbon spacers to design a series of novel 1-hydroxyl-3-aminoalkoxy thioxanthone derivatives (**Figure 2**). In this article, these new compounds were synthesized and evaluated for their biological activities, including AChE, MAOs and Aβ aggregation inhibitory activities, antioxidant and metal chelating effects.

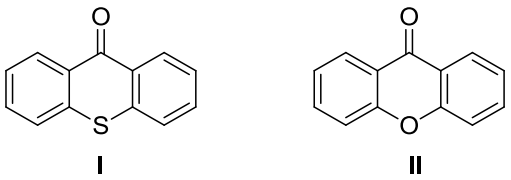

Figure 1. Structures of thioxanthone (**I**) and xanthone (**II**)

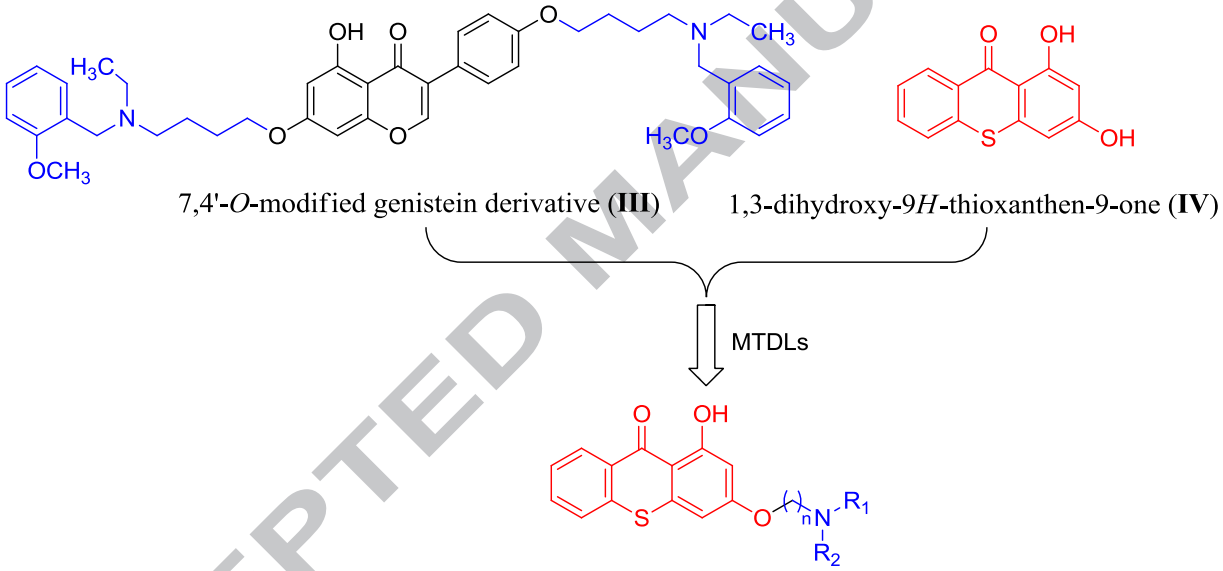

Figure 2. Design strategy for 1-hydroxyl-3-aminoalkoxythioxanthone derivatives.

2. Results and discussion

2.1. Chemistry

The general route for the synthesis of 1-hydroxyl-3-aminoalkoxythioxanthone derivatives was shown in **Scheme 1**. 2,2'-disulfanediyldibenzoic acid (**1**) was prepared according to the literature using 2-aminobenzoic acid as a starting material.[30] 1,3-dihydroxy-9*H*-thioxanthen-9-one (**2**) was synthesized in a yield of 46.4% via the cyclization of **1** and phloroglucinol in the presence of Eaton's reagent.[31,32] Then, 3-hydroxyl group of compound **2** was alkylated in the presence of K_2CO_3 by the addition of two equivalent amounts of 1,3-dibromopropane, 1,4-dibromobutane or

1,6-dibromohexane to give the key intermediates **3-5** respectively.[32,33] Due to the hydrogen bond between 1-hydroxyl and 9-carbonyl group, the reactivity of 1-hydroxyl group was much lower than 3-hydroxyl group and 3-alkylated products were obtained exclusively[32]. Finally, compound **3-5** were reacted with corresponding secondary amines **6a-f** to afford the target compounds **7a-f**, **8a-f**, and **9a-f**.[29] All the thioxanthone derivatives were characterized by ^{1}H NMR, ^{13}C NMR and ESI-MS.

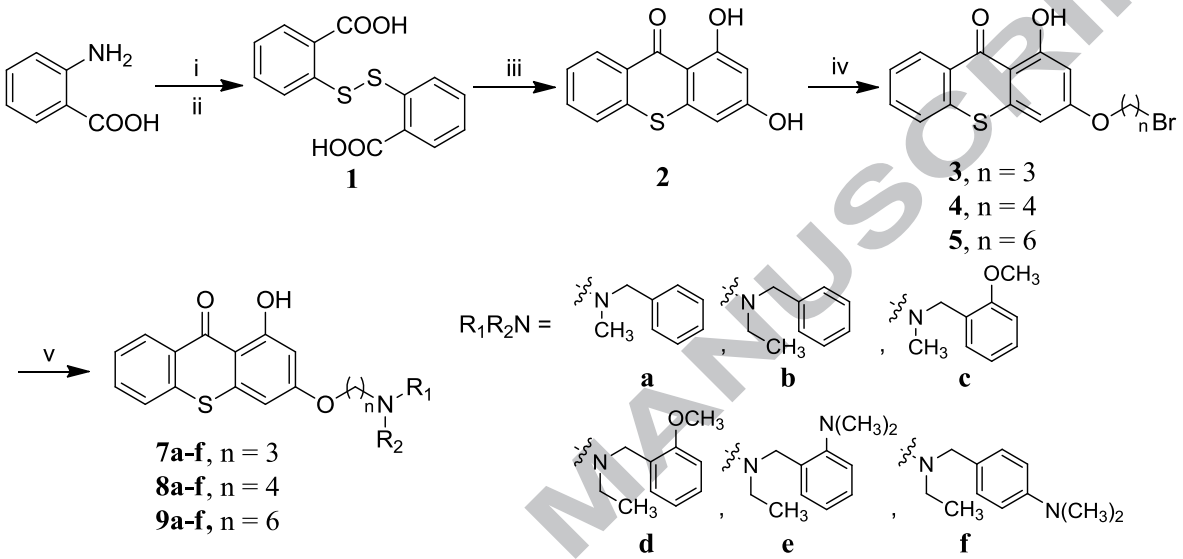

Scheme 1. Synthesis of thioxanthone derivatives **7-9**. *Reagents and conditions:* (i) $NaNO_2$, *conc.*HCl, H_2O, 5 °C for 20 min; (ii) $Na_2S{\cdot}9H_2O$, S, NaOH, 0-5 °C, then r.t. for 2 h; (iii) Phloroglucinol, P_2O_5, CH_3SO_3H, 90 °C for 1.5 h; (iv) $Br(CH_2)_nBr$, K_2CO_3, acetone, reflux for 5-7 h; (v) NHR_1R_2 (**6a-f**), K_2CO_3, CH_3CN, reflux for 4-9 h.

2.2. Pharmacology

2.2.1. Inhibition studies on AChE and BuChE

The inhibitory activities of all the synthesized derivatives against AChE from *Electrophorus electricus* (*Ee*AChE) and BuChE from rat serum (*Rat*BuChE) were determined by modified Ellman's method[34], using donepezil as a reference compound. The target compounds showed inhibitory activity against AChE with IC_{50} values ranging from submicromolar to micromolar. As shown in **Table 1**, all target compounds showed much more AChE inhibitory potency than the lead compound **2** (IC_{50} = 38.90 ± 0.85 μM), which indicated that the introduction of the *O*-alkylbenzylamine group was beneficial. Among them, compounds **7e**, **9a**, **9b** and **9e** exhibited excellent efficiency to inhibit AChE (IC_{50} = 0.25 ± 0.01 μM, 0.32 ± 0.02 μM, 0.58 ± 0.03 μM, 0.59 ± 0.02 μM, respectively).

Moreover, the AChE inhibitory potency was related to the length of alkylene spacer chains. In general, the derivatives with a 6-methylene linker showed better inhibition of AChE than those with a 3- or 4-methylene chain. For example, compounds **9a-c** (n = 6) were much more potent than compounds **7a-c** (n = 3) and **8a-c** (n = 4). Compared with **9a** (n = 6, IC_{50} = 0.32 ± 0.02 μM), the AChE inhibitory activity of **8a** (n = 4) was about 39-fold lower (IC_{50} = 12.41 ± 0.29 μM), and **7a** (n = 3) was almost 35-fold lower (IC_{50} = 11.20 ± 0.24 μM). Therefore, the alkyl chain with 6-methylene may be optimal for the inhibition of AChE. It also revealed that the various benzylamine moieties were closely related to the inhibitory activity. Compounds possessing an *N*-methyl group usually displayed better AChE inhibitory activity than those with an *N*-ethyl group (AChE inhibitory activity: **7a** > **7b**, **8a** > **8b**, **9a** > **9b**). Furthermore, the adoption of 2-dimethylamino group on the benzylamine moiety dramatically improved AChE inhibitory activity (**7e**, **8e** and **9e**; IC_{50} = 0.25 ± 0.01 μM, 2.88 ± 0.07 μM and 0.59 ± 0.02 μM, respectively), while the introduction of 4-dimethylamino group significantly decreased the potency (**7f**, **8f** and **9f**; IC_{50} = 17.70 ± 0.56 μM, 25.40 ± 0.94 μM and 33.80 ± 0.98 μM, respectively). In contrast, the adoption of 2-methoxy group showed no obvious regularity. Overall, the results suggested that *N*-benzylmethylamine and *N*-(2-dimethylaminobenzyl) ethylamine might be more appropriate for AChE inhibition. Almost all compounds exhibited weak activity against BuChE. This result showed that these derivatives were potent high selective AChE inhibitors. This selectivity profile was a limitation to some extent, but it might be beneficial to diminish peripheral cholinergic side effects and provide lower toxicity. A typical case in point is tacrine, which had severe side effects because of its poor selectivity.[35] Based on the above results, compound **9e** was selected for kinetic analysis to investigate the type of inhibition.

Table 1. Inhibition of AChE, BuChE and MAOs activities by compound **2** and its derivatives, reference compounds and 7,4′-*O*-modified genistein derivative (**III**).

Compound	IC_{50}(μM) ± SD[a] *Ee*AChE[b]	Inhibition(%)[c] *Rat*BuChE	IC_{50}(μM) ± SD		SI[d]
			MAO-A	MAO-B	
7a	11.20 ± 0.24	n.a.[e]	16.00 ± 0.63	1.73 ± 0.03	9.25
7b	18.40 ± 0.49	31.8 ± 0.74	13.20 ± 0.59	7.13 ± 0.32	1.85
7c	28.70 ± 0.98	30.2 ± 0.56	6.31 ± 0.12	6.09 ± 0.19	1.04
7d	2.79 ± 0.13	17.3 ± 0.27	8.17 ± 0.23	1.88 ± 0.07	4.35

7e	0.25 ± 0.01	22.4 ± 0.54	5.94 ± 0.21	3.73 ± 0.15	1.59
7f	17.70 ± 0.56	n.a.[e]	2.79 ± 0.14	3.55 ± 0.09	0.79
8a	12.41 ± 0.29	n.a.[e]	0.57 ± 0.03	0.37 ± 0.02	1.54
8b	22.00 ± 0.83	n.a.[e]	0.34 ± 0.02	0.27 ± 0.01	1.26
8c	9.16 ± 0.36	5.62 ± 0.24	0.62 ± 0.03	0.59 ± 0.02	1.05
8d	15.50 ± 0.49	n.a.[e]	1.02 ± 0.06	0.88 ± 0.03	1.16
8e	2.88 ± 0.07	30.3 ± 0.89	1.54 ± 0.04	2.02 ± 0.11	0.76
8f	25.40 ± 0.94	7.15 ± 0.42	1.00 ± 0.02	2.20 ± 0.08	0.45
9a	0.32 ± 0.02	n.a.[e]	0.57 ± 0.01	0.35 ± 0.02	1.63
9b	0.58 ± 0.03	8.83 ± 0.31	1.44 ± 0.06	0.33 ± 0.01	4.36
9c	4.28 ± 0.19	14.9 ± 0.76	1.03 ± 0.02	0.38 ± 0.01	2.71
9d	11.50 ± 0.51	13.9 ± 0.42	1.30 ± 0.03	0.46 ± 0.03	2.83
9e	0.59 ± 0.02	28.7 ± 0.54	1.01 ± 0.02	0.90 ± 0.01	1.12
9f	33.80 ± 0.98	n.a.[e]	1.25 ± 0.09	0.39 ± 0.03	3.21
2	38.90 ± 0.85	n.a.[e]	0.28 ± 0.01	0.30 ± 0.02	0.93
III	0.14 ± 0.003	20.0	—	—	—
Donepezil	0.0226 ± 0.0010	IC_{50} = 21.4 ± 0.97 μM	—	—	—
Clorgyline	—	—	0.0027 ± 0.0005	2.43 ± 0.11	0.00112
Rasagiline	—	—	2.61 ± 0.02	0.00997 ± 0.00072	261.79
Iproniazid	—	—	0.837 ± 0.012	0.985 ± 0.025	0.85

[a] IC_{50} values represent the concentration of inhibitor required to decrease enzyme activity by 50% and are the mean of three independent experiments, each performed in triplicate. Data were expressed as mean ± SD (SD = standard deviation).

[b] From *Electrophorus electricus*.

[c] BuChE from rat serum and tested compounds were used at 50 μM.

[d] SI = IC_{50} (MAO-A) / IC_{50} (MAO-B).

[e] n.a. = no active. Compounds defined "no active" means that percent inhibition is less than 5.0% at a concentration of 50 μM in the assay conditions.

2.2.2. Kinetic study for the inhibition of AChE

In order to investigate the inhibitory mechanism for this family of compounds toward AChE, a

kinetic study was performed with compound **9e** by using *Ee*AChE. The Lineweaver-Burk reciprocal plots (**Figure 3**) indicated that with increasing concentrations of **9e**, both the slopes (decreased V_{max}) and intercepts (higher K_m) were increased. This pattern revealed a mixed-type inhibition, which implied that compound **9e** was likely to bind both of the CAS and PAS of AChE.

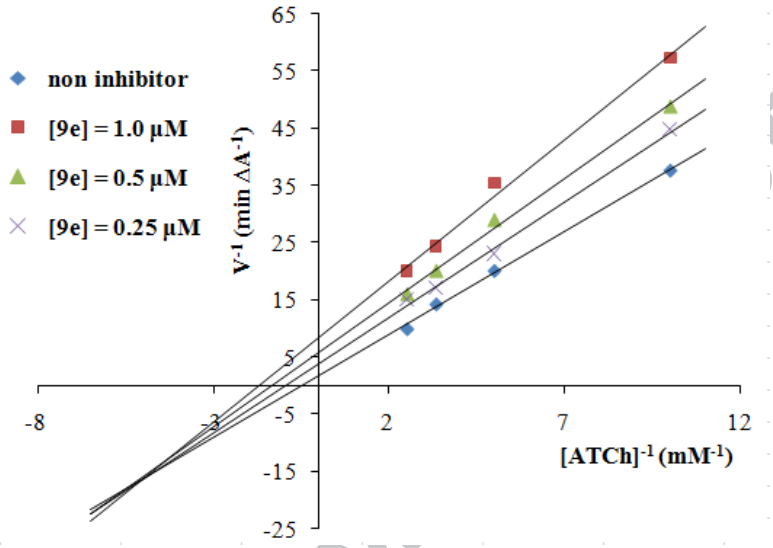

Figure 3. Kinetic study on the mechanism of *Ee*AChE inhibition by compound **9e**. Merged Lineweaver-Burk reciprocal plots of AChE initial velocity with increasing substrate concentration (0.1-0.4 mM) in the absence or presence of **9e**. Lines were derived from a weighted least-squares analysis of data points.

2.2.3. Molecular modeling study of AChE

To clarify the binding modes between thioxanthone derivatives and AChE, a molecular modeling study was carried out using the docking program, AutoDock 4.2 package with Discovery Studio 2.5, based on the X-ray crystal structure of *Torpedo californica (Tc)* AChE (PDB: 1EVE).[36-38] Considering the result of AChE inhibition assay and the kinetic study, compound **9e** was chosen for our molecular modeling investigation. Due to the flexible structure of **9e**, there were many conformational clusters, most of which showed the binding energy with -12 to -11 kcal/mol. Took into account the binding energy and the conformational distribution, the most stable binding mode was graphically inspected (**Figure 4**, binding energy: -12.34 kcal/mol, inhibit constant: 0.904 nM). As shown in **Figure 4**, **9e** occupied the entire enzymatic CAS, the mid-gorge sites and PAS. One hydrogen bond was generated between the ligand **9e** and the residue Arg289 (Arg289=O • • • HO-**9e**).

The long chain of methylene folded in a conformation in the gorge that allowed it to interact with Tyr334, Phe330 and Phe331via the hydrophobic interaction. Moreover, the benzylamine moiety of **9e** was observed to adopt a parallel π-π interaction with Trp84. The docking study indicated that **9e** could stably bind to the CAS and PAS of AChE, consistent with our kinetic analysis result.

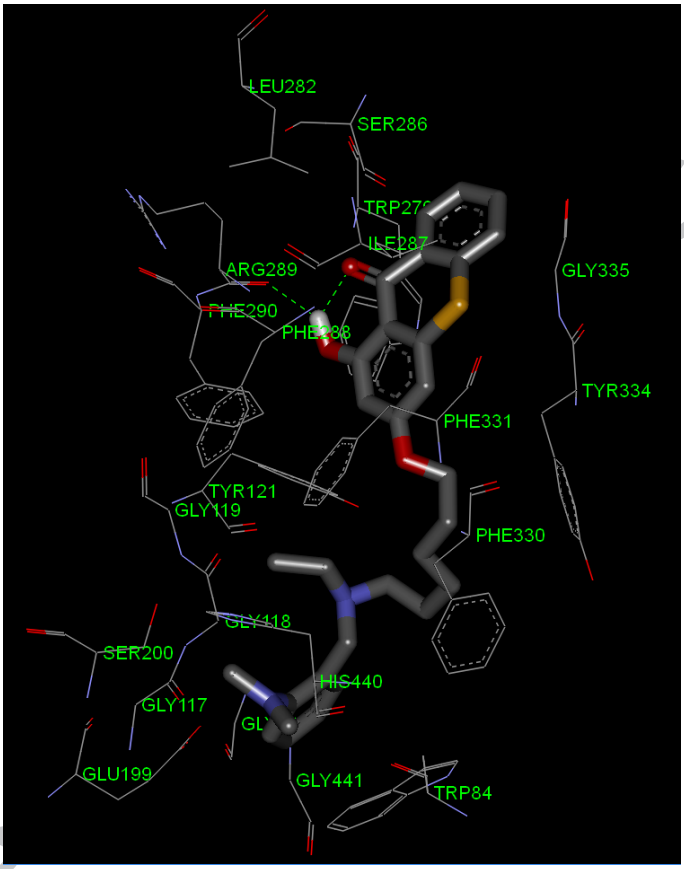

Figure 4. Docking pose of compound **9e** (colored by atom type) into the binding site of *Tc*AChE (PDB: 1EVE), highlighting the protein residues that participate in the main interactions with the inhibitor. Picture was generated with Discovery Studio 2.5. (For interpretation of the references to color in this figure legend, the reader is referred to the web version of this article.)

2.2.4. Inhibition studies on recombinant human MAO-A and -B

The inhibitory activity against human MAO-A and -B was measured using clorgyline, iproniazid and rasagiline as reference compounds. As shown in **Table 1**, most of these compounds were effective in inhibiting MAO in submicromolar range, retaining the activities of the lead compound **2** (IC_{50} = 0.28 ± 0.01 μM to MAO-A, 0.30 ± 0.02 μM to MAO-B). Among them, compound **8b** was the most potent inhibitor for both MAO-A and -B with IC_{50} values of 0.34 ± 0.02 μM and 0.27 ± 0.01 μM, respectively. The results exhibited that the derivatives with a 3-methylene

linker were less active than those with a 4- or 6-methylene chain. Besides, the structure-activity relationship analysis indicated that the inhibitory potency of MAO-B rose as the length of chain increased (such as **7e**, **8e** and **9e**; IC_{50} = 3.73 ± 0.15 μM, 2.02 ± 0.11 μM and 0.90 ± 0.01 μM, respectively), but this conclusion for MAO-A was different. It also revealed that compounds bearing various benzylamine moieties showed no significant difference on MAO inhibitory potency.

2.2.5. Molecular modeling study of MAOs

The interaction mode of these target compounds to MAOs were performed based on the X-ray crystal structures of human MAO-A (PDB: 2Z5X) and MAO-B (PDB: 2V60). From the results of inhibition studies on AChE and MAOs, compound **9e** was chosen as a representative for the molecular modeling investigation. The most stable binding modes of **9e** in MAO-A and -B active sites were graphically inspected (**Figure 5**). As shown in **Figure 5A**, the thioxanthone ring was close to the enzymatic cofactor FAD in MAO-A. One hydrogen bond was generated between the ligand **9e** and FAD (**9e**-OH • • • O=C-FAD). Furthermore, the thioxanthone ring was observed to adopt parallel π-π interactions with Tyr407 and Tyr444. In **Figure 5B**, the thioxanthone ring was located far from the FAD in MAO-B. Two hydrogen bonds were formed between the 1-OH of **9e** and the active site of MAO-B (Ile199=O • • • HO-**9e**; Tyr326-OH • • • O-**9e**). In addition, the benzylamine moiety of **9e** interacted with Tyr398 and Tyr435 via parallel π-π interactions. Therefore, the docking studies explained the high MAO inhibitory activity of these derivatives, which consistent with the conclusion resulting from the human MAO inhibition assay.

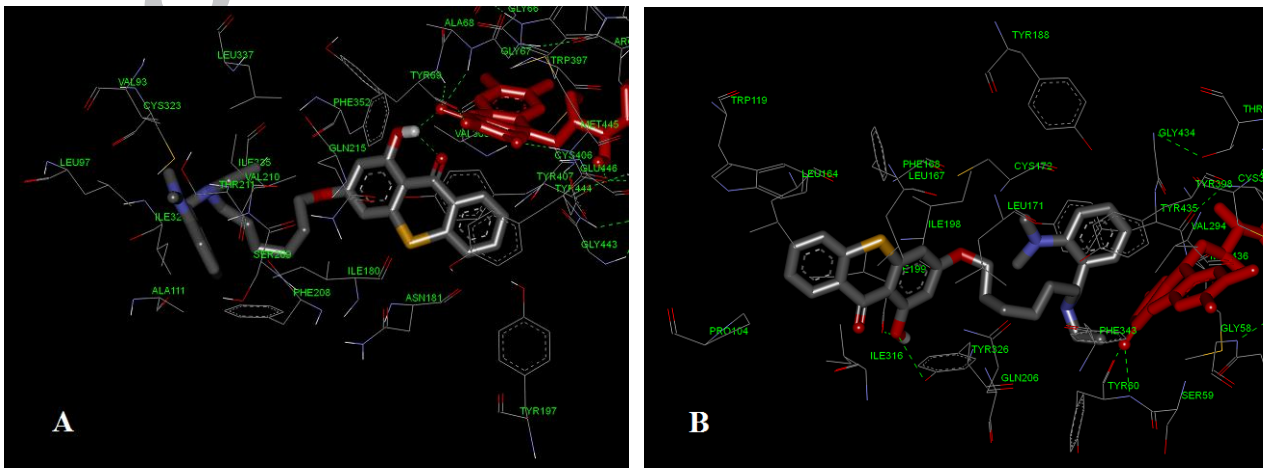

Figure 5. Representation of compound **9e** docked into the binding sites of MAO-A (**A**) and -B (**B**), highlighting the protein residues that participate in the main interactions with the inhibitor. Ligand **9e**

and FAD are displayed in grey and red respectively. Hydrogen-bonds are shown with the green dotted lines. Picture was generated with Discovery Studio 2.5. (For interpretation of the references to color in this figure legend, the reader is referred to the web version of this article.)

2.2.6. Inhibition of self- and Cu^{2+}-induced Aβ_{1-42} aggregation

All synthesized compounds were tested for their ability to inhibit self- and Cu^{2+}-induced Aβ_{1-42} aggregation by using thioflavin T fluorescence method.[39,40] Curcumin was used as the reference compound. The results summarized in **Table 2** indicated that these derivatives exhibited excellent inhibitory activities of both self- and Cu^{2+}-induced Aβ_{1-42} aggregation. Furthermore, the representative compound **9e** exhibited good inhibitory potency of self- and Cu^{2+}-induced Aβ_{1-42} aggregation with the percentage of 74.8 ± 1.2% and 87.7 ± 1.9%, respectively. Compared with lead compound **2** (9.5 ± 0.3% and 31.4 ± 1.2% respectively), the introduction of the *O*-alkylbenzylamine group greatly increased Aβ_{1-42} aggregation inhibitory efficiency. For the inhibition of self-induced Aβ_{1-42} aggregation, compound **8d** (n = 4) exhibited the highest inhibitory activity with inhibitory percentage of 89.4 ± 2.1%. Interestingly, compound **7d** (68.2 ± 4.3%) and **9d** (78.7 ± 3.5%) exhibited the highest inhibitory activity among the derivatives with a 3-methylene linker and 6-methylene linker, respectively. It revealed that compounds **7d**, **8d** and **9d** featuring a *N*-(2-methoxybenzyl)ethylamine group on the terminal side of carbon chain may be optimal for the inhibition of self-induced Aβ_{1-42} aggregation. Regarding the inhibition of Cu^{2+}-induced Aβ_{1-42} aggregation, compounds that featuring a *N*-(4-dimethylaminobenzyl)ethylamine group on the terminal side of carbon chain may be beneficial for the inhibition of Cu^{2+}-induced Aβ_{1-42} aggregation. For example, **7f** (85.4 ± 4.3%) and **9f** (91.3 ± 4.7%) exhibited the highest inhibitory activity among the derivatives with a 3-methylene and 6-methylene linker, respectively. Generally, almost all the compounds exhibited better inhibitory activities of Cu^{2+}-induced Aβ_{1-42} aggregation than that of self-induced Aβ_{1-42} aggregation. This result might be reasonably attributed to the chelating effect, which greatly reduced the speed and degree of Cu^{2+}-induced Aβ_{1-42} aggregation. Besides, the results also showed that the derivatives with a 4-methylene linker possessed better inhibitory activities than those with a 3- or 6-methylene chain, which were different from the conclusion of AChE inhibition assays. Therefore, the length of the alkyl chain also played an important role in inhibiting the aggregation of Aβ_{1-42}.

Table 2. Inhibition of self- and Cu^{2+}-induced Aβ_{1-42} aggregation activities, oxygen radical absorbance capacity (ORAC, Trolox equivalents) by compound **2** and its derivatives, reference compounds and 7,4′-*O*-modified genistein derivative (**III**).

Compound	% Inhibition of Aβ_{1-42} aggregation[a]		ORAC[d]
	Self-induced[b]	Cu^{2+}-induced[c]	
7a	40.5 ± 1.6	81.1 ± 2.9	0.48 ± 0.01
7b	46.9 ± 2.1	70.9 ± 1.5	0.59 ± 0.03
7c	45.2 ± 2.6	77.8 ± 3.9	0.22 ± 0.01
7d	68.2 ± 4.3	80.0 ± 2.1	0.68 ± 0.02
7e	46.9 ± 1.1	75.7 ± 3.1	0.35 ± 0.01
7f	64.8 ± 2.1	85.4 ± 4.3	1.38 ± 0.10
8a	79.5 ± 4.5	88.6 ± 2.0	1.18 ± 0.09
8b	75.8 ± 1.2	82.1 ± 3.9	1.00 ± 0.08
8c	79.9 ± 2.0	88.0 ± 2.3	1.04 ± 0.05
8d	89.4 ± 2.1	82.0 ± 2.7	0.57 ± 0.04
8e	72.1 ± 1.8	82.1 ± 4.2	0.95 ± 0.06
8f	77.1 ± 1.3	81.9 ± 6.5	1.50 ± 0.11
9a	47.5 ± 2.6	76.8 ± 1.8	0.37 ± 0.03
9b	50.6 ± 2.7	76.4 ± 2.8	0.17 ± 0.01
9c	68.0 ± 3.2	86.5 ± 2.3	0.66 ± 0.02
9d	78.7 ± 3.5	86.3 ± 3.0	0.83 ± 0.07
9e	74.8 ± 1.2	87.7 ± 1.9	0.74 ± 0.02
9f	76.3 ± 3.1	91.3 ± 4.7	1.37 ± 0.05
2	9.5 ± 0.3	31.4 ± 1.2	0.42 ± 0.02
III	35.0 ± 1.0	77.8 ± 4.0	0.30 ± 0.01
Curcumin	36.2 ± 0.9	70.0 ± 2.7	2.43 ± 0.04

[a] For inhibition of Aβ aggregation, the thioflavin-T fluorescence method was used.

[b] Inhibition of self-induced Aβ_{1-42} aggregation by tested inhibitors at 25 μM.

[c] Inhibition of Cu^{2+}-induced Aβ_{1-42} aggregation. The concentration of tested compounds and Cu^{2+} were 25 μM.

[d] The mean ± SD of the three independent experiments. Data are expressed as μM of Trolox equivalent/μM of tested compound.

2.2.7. Evaluation for antioxidant activity

The antioxidant activities of these derivatives were evaluated by the ORAC-FL method[41] and the results were summarized in **Table 2**. Their ability to scavenge radicals was provided as a Trolox (a vitamin E analog) equivalent, with their relative potency at 5 μM compared with Trolox. The antioxidant capacity of these compounds was determined by their competition with fluorescein in the radical capture, using a fluorescence microplate reader. Most of the target compounds demonstrated moderate to good antioxidant activities compared to Trolox. Curcumin, as another reference, possessed better antioxidant activity because that contained two phenolic hydroxyl groups and could tautomerize to enol form. Among these tested compounds, **7f**, **8f** and **9f** showed the most potent antioxidant activity of this family with ORAC-FL values of 1.38 ± 0.10, 1.50 ± 0.11 and 1.37 ± 0.05 Trolox equivalents, respectively. It revealed that the *N*-(4-dimethylaminobenzyl) ethylamine moiety seemed to be a potent substitution pattern to improve the antioxidant activity. However, the length of the linker did not show distinct influence on the potency.

2.2.8. Studies of metal-chelating properties

Based on the above studies, metal-chelating properties of these derivatives toward biometals such as Cu^{2+}, Zn^{2+}, Fe^{2+} and Al^{3+} were studied by ultraviolet-visible (UV-Vis) spectrometry, with **9e** as the representative compound. The spectrum of **9e** was shown in **Figure 6A**. When $CuCl_2$ was added, red shifts occurred in the absorption wavelength from 302 nm and 324 nm to 330 nm and 342 nm, respectively. Interestingly, the maximum absorption at 264 nm exhibited a blue shift to 255 nm, and the absorbance dropped significantly. These results indicated the formation of a **9e**-Cu^{2+} complex. When $FeSO_4$ was added, the spectrum changed significantly, and the absorbance increased obviously, suggesting a possible interaction between **9e** and Fe^{2+}. However, no significant change was observed with the addition of $AlCl_3$ or $ZnCl_2$. The chelating effect could be reasonably attributed to the 9-carbonyl and 1-hydroxyl group at the thioxanthone[25] as well as the benzylamine moiety side-chain. And it also explained the high potency of the derivatives to block the Cu^{2+}-induced $A\beta_{1\text{-}42}$ aggregation.

The stoichiometry of **9e**-Cu^{2+} complex was determined using the molar ratio method, by preparing the methanol solutions of compound **9e** with increasing amounts of $CuCl_2$. The UV spectra was used to obtain the absorbance of the **9e** complex at different concentrations of $CuCl_2$ at 342 nm. The results showed that absorbance linearly increased initially and then plateaued (**Figure 6B**). The

two straight lines intersected at a mole fraction of 1.50, revealing a 1:1.5 stoichiometry for complex **9e**-Cu^{2+}.

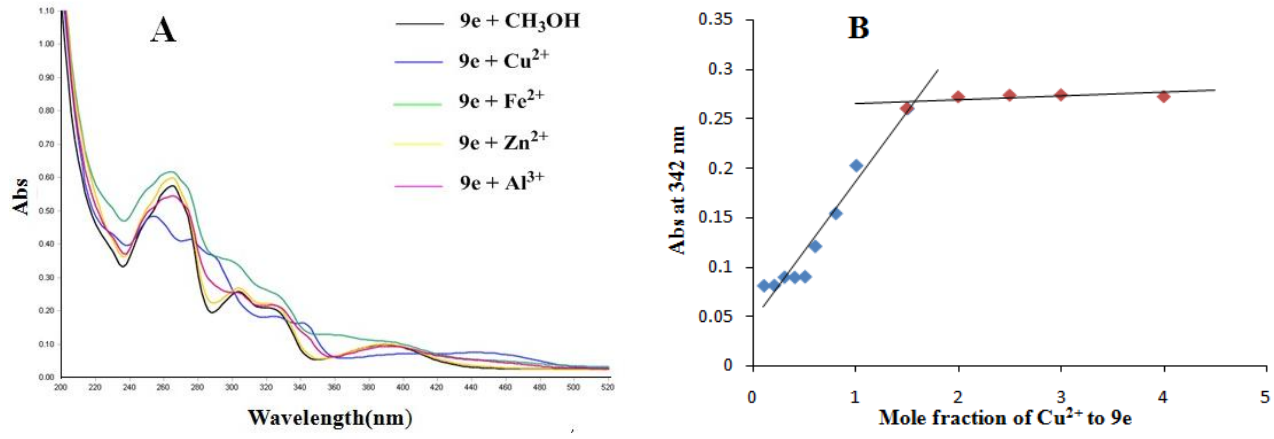

Figure 6. (**A**) UV spectrum of compound **9e** (37.5 µM in methanol) alone or in the presence of $CuCl_2$, $FeSO_4$, $ZnCl_2$ or $AlCl_3$ (37.5 µM for all metals in methanol). (**B**) Determination of the stoichiometry of complex-Cu^{2+} by using the molar ratio method of titrating the methanol solution of compound **9e** with ascending amounts of $CuCl_2$. The final concentration of tested compound was 37.5 µM, and the final concentration of Cu^{2+} ranged from 3.75 to 150 µM.

2.2.9. Cytotoxic effect on SH-SY5Y cells

To examine the cytotoxicity of the representative compound **9e**, the human neuronal cell line SH-SY5Y cells were treated with **9e** at three different concentrations (1, 10 and 100µM) for 24 h. The cell viability was determined by the 3-(4,5-dimethylthiazol-2-yl)-2,5-diphenyltetrazolium (MTT) assays[42,43]. As shown in **Figure 7**, cell viability reached 99.7% and 96.8% when **9e** was tested at 1 µM and 10 µM, respectively. With increased concentration to 100 µM, **9e** exhibited a decrease of cell viability (68.1%). These results showed that compound **9e** had a wide therapeutic safety range.

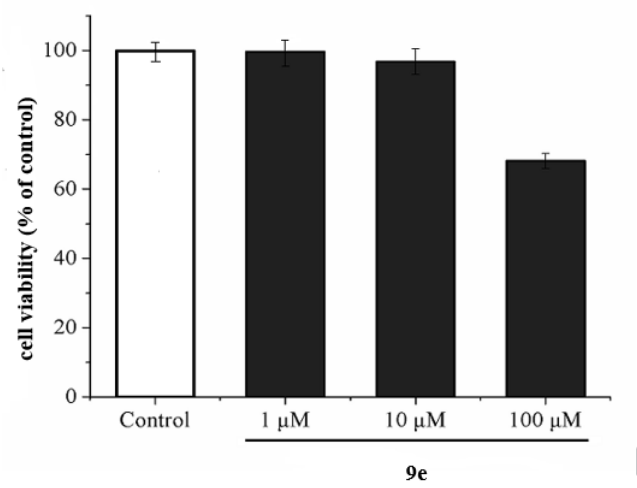

Figure 7. Effect of compound **9e** on cell viability in human SH-SY5Y cells. Data are mean values ± SEM of three independent experiments.

2.2.10. *In vitro* blood-brain barrier permeation assay

The ability to cross the blood-brain barrier (BBB) and penetrate into the brain is an important property for compounds in the treatment of AD. The parallel artificial membrane permeation assay of the blood-brain barrier (PAMPA-BBB) was conducted to predict the *in vivo* BBB permeability of our derivatives[44,45]. Compounds **9b** and **9e** were chosen as representatives for BBB permeation assay. To validate the assay, the experimental permeabilities of 11 commercial drugs were compared with reported values (**Table 3**). And a plot of experimental data versus the bibliographic values displayed a good linear correlation: P_e (exp.) = 0.8792 × P_e (bibl.) − 0.0616 (R^2 = 0.9555) (**Figure 8**). With the consideration of the limit established by Di *et al.*[44], we determined that compounds with P_e values above 3.46 × 10^{-6} cm/s could cross the BBB (**Table 4**). The results in **Table 5** indicated that compound **9b** and **9e** could penetrate the BBB and reach the therapeutic targets in central nervous system (CNS).

Table 3. Permeability P_e (× 10^{-6} cm/s) in the PAMPA-BBB assay for 11 commercial drugs used in the experiment validation.

Commercial drugs	Bibl[a]	PBS/EtOH (70:30)[b]
Verapamil	16	16.20 ± 0.36
Oxazepam	10	9.20 ± 0.21
Diazepam	16	10.90 ± 0.23
Clonidine	5.3	5.50 ± 0.16
Imipramine	13	11.20 ± 0.22
Testosterone	17	15.50 ± 0.25

Caffeine	1.3	1.22 ± 0.05
Enoxacine	0.9	0.55 ± 0.01
Piroxicam	2.5	0.84 ± 0.02
Norfloxacin	0.1	0.33 ± 0.01
Theophylline	0.12	0.17 ± 0.03

[a] Taken from Ref.[44].

[b] Data are the mean ± SD of three independent experiments.

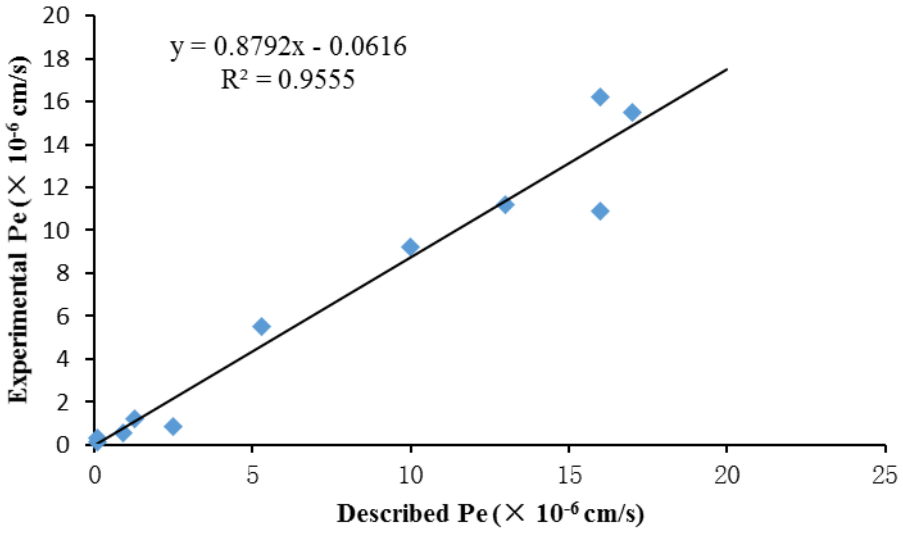

Figure 8. Lineal correlation between experimental and reported permeability of commercial drugs using the PAMPA-BBB assay. P_e (exp.) = 0.8792 × P_e (bibl.) − 0.0616 (R^2 = 0.9555)

Table 4. Ranges of permeability of PAMPA-BBB assays (P_e × 10^{-6} cm/s).

High BBB permeation predicted (CNS +)	$P_e > 3.46$
Uncertain BBB permeation (CNS +/-)	$3.46 > P_e > 1.70$
Low BBB permeation predicted (CNS -)	$P_e < 1.70$

Table 5. Permeability results P_e (× 10^{-6} cm/s) from the PAMPA-BBB assay for selected thioxanthone derivatives with their predicted penetration into the CNS.

Compd.[a]	P_e (× 10^{-6} cm/s)[b]	Prediction
9b	4.12 ± 0.18	CNS +
9e	3.49 ± 0.34	CNS +

[a] Compounds were dissolved in tartaric acid aqueous solution and diluted with PBS/EtOH (70:30). The final concentration of each compound was 100 μg/mL.

[b] Data are the mean ± SD of three independent experiments.

3. Conclusion

In summary, most of these 1-hydroxyl-3-aminoalkoxythioxanthone derivatives exhibited good AChE and MAOs inhibitory activities, significant efficiency to block both self- and Cu^{2+}-induced A$\beta_{1\text{-}42}$ aggregation, and moderate to good antioxidant activities. Overall, compound **9e** displayed excellent and balanced activities: AChE (IC_{50} = 0.59 ± 0.02 μM), MAO-A and MAO-B (IC_{50} = 1.01 ± 0.02 μM and 0.90 ± 0.01 μM respectively), self- and Cu^{2+}-induced A$\beta_{1\text{-}42}$ aggregation (74.8 ± 1.2% and 87.7 ± 1.9% at 25 μM, respectively), good metal-chelating properties and low toxicity in SH-SY5Y cells. Furthermore, kinetic and molecular modeling studies indicated that compound **9e** showed a mixed-type inhibition, binding to both CAS and PAS of AChE, and could penetrate the BBB. Therefore, according to the MTDLs strategy, the multifunctional properties made **9e** a promising candidate for further studies directed to the development of novel drugs in the treatment of AD.

4. Experimental section

4.1. Chemistry

All chemical reagents and solvents were obtained from commercial sources and used without further purification. Melting points were determined on YRT-3 melting-point apparatus (China) and are uncorrected. Reactions were monitored by thin-layer chromatography (TLC) on silica gel GF_{254} plates from Qingdao Haiyang Chemical Co. Ltd. (China) and spots were visualized with UV lamp (254 nm) or in iodine chamber. ^{1}H NMR and ^{13}C NMR spectra were recorded on a Varian INOVA 400 NMR spectrometer or Varian INOVA 600 NMR spectrometer at room temperature using $CDCl_3$ or DMSO-d_6 as the sovent. Chemical shifts were expressed in parts per millions (ppm) using tetramethylsilane (TMS) as the internal standard. Coupling constants were reported in hertz. Column chromatography was accomplished on silica gel (230-400 mesh) purchased from Qingdao Haiyang Chemical Co. Ltd. (China). The purity of these compounds was determined by analytical reverse phase high-performance liquid chromatography (HPLC) on a Shimadzu LC-10Avp plus system with a Kromasil C18 column (4.6 mm×250 mm, 5μm). The mobile phase was a mixture of methanol and water (both containing 0.1% formic acid) at a flow rate of 0.7 mL/min. All target compounds possessed purity higher than 95%. MS spectra were performed on Agilent-627 TOF LC-MS

Spectrometer.

4.1.1. Synthesis of 2,2'-disulfanediyldibenzoic acid (1)

2,2'-disulfanediyldibenzoic acid (**1**) was prepared according to the literature,[30] which was used without further purification. 95.8% yield.

4.1.2. Synthesis of 1,3-dihydroxy-9*H*-thioxanthen-9-one (2)

A mixture of phosphorous pentoxide (4.13 g, 29.1 mmol) and methanesulfonic acid (30 mL) was heated to 90 ℃ and stirred for 0.5 h under an argon atmosphere until a clear solution (Eaton's reagent) was obtained. Anhydrous phloroglucinol (1.11 g, 8.79 mmol) and 2,2'-disulfanediyldibenzoic acid (**1**, 1.14 g, 3.63 mmol) were then added in one portion. The reaction mixture was stirred at 90 ℃ for 1.5 h. After cooling to room temperature, the reaction mixture was poured into ice-water and stirred for 1 h at room temperature. The resulting solid was collected by filtration, washed with water to adjust the pH to approximately 6, and dried at 70 ℃ to give **2** as a reddish brown solid. The crude product was purified by silica gel column chromatography using petroleum ether/ethyl acetate (12:1, v/v) as eluent to obtain compound **2** (1.03 g, 46.4%) as a yellow solid. ^{1}H NMR (400 MHz, DMSO-d_6) δ 14.37 (s, 1H), 11.10 (s, 1H), 8.43 (d, J = 7.6 Hz, 1H), 7.80-7.72 (m, 2H), 7.60-7.54 (m, 1H), 6.65 (s, 1H), 6.32 (s, 1H).

4.1.3. General procedure for the synthesis of (3-5)

To a mixture of 1,3-dihydroxy-9*H*-thioxanthen-9-one (**2**, 300 mg, 1.23 mmol) and anhydrous potassium carbonate (170 mg, 1.23 mmol) in acetone (5 mL), appropriate dibromoalkane derivative (2.46 mmol) was added. The reaction mixture was refluxed for 5-7 h under an argon atmosphere until the starting material disappeared, the solvent was evaporated under reduced pressure. Water (20 mL) was added to the oil residue and the mixture was extracted with dichloromethane (15 mL × 4). The combined organic phases were washed with saturated aqueous sodium chloride (30 mL), dried over sodium sulfate and filtered, concentrated under reduced pressure to obtain crude compound. The residue was purified by silica gel chromatography using petroleum ether/ethyl acetate (30:1) as eluent to afford the desired products **3-5**.

4.1.3.1. 3-(3-bromopropoxy)-1-hydroxy-9*H*-thioxanthen-9-one (3)

It was synthesized from 1,3-dihydroxy-9*H*-thioxanthen-9-one (**2**) and 1,3-dibromopropane according to the general procedure. 77.3% yield; yellow solid; mp 131.1-132.8 ℃. ^{1}H NMR (400 MHz, $CDCl_3$) δ 14.44 (s, 1H), 8.55 (dd, J = 1.2, 8.4 Hz, 1H), 7.60 (t, J = 8.4 Hz, 1H), 7.48 (t, J = 8.4

Hz, 1H), 7.45 (d, *J* = 8.4 Hz, 1H), 6.57 (d, *J* = 2.4 Hz, 1H), 6.44 (d, *J* = 2.4 Hz, 1H), 4.20 (t, *J* = 6.0 Hz, 2H), 3.61 (t, *J* = 6.4 Hz, 2H), 2.38−2.32 (m, 2H).

4.1.3.2. 3-(4-bromobutoxy)-1-hydroxy-9*H*-thioxanthen-9-one (4)

It was synthesized from 1,3-dihydroxy-9*H*-thioxanthen-9-one (**2**) and 1,4-dibromobutane according to the general procedure. 80.4% yield; yellow solid; mp 118.9-120.4 °C. ^{1}H NMR (400 MHz, $CDCl_3$) δ 14.44 (s, 1H), 8.55 (dd, *J* = 1.2, 8.0 Hz, 1H), 7.59 (t, *J* = 8.0 Hz, 1H), 7.48 (t, *J* = 8.0 Hz, 1H), 7.46 (d, *J* = 8.0 Hz, 1H), 6.55 (d, *J* = 2.4 Hz, 1H), 6.42 (d, *J* = 2.4 Hz, 1H), 4.08 (t, *J* = 6.0 Hz, 2H), 3.50 (t, *J* = 6.4 Hz, 2H), 2.11−2.04 (m, 2H), 2.01−1.95 (m, 2H).

4.1.3.3. 3-((6-bromohexyl)oxy)-1-hydroxy-9*H*-thioxanthen-9-one (5)

It was synthesized from 1,3-dihydroxy-9*H*-thioxanthen-9-one (**2**) and 1,6-dibromohexane according to the general procedure. 83.1% yield; yellow solid; mp 101.6-103.2 °C. ^{1}H NMR (400 MHz, $CDCl_3$) δ 14.45 (s, 1H), 8.55 (d, *J* = 8.0 Hz, 1H), 7.60 (t, *J* = 8.0 Hz, 1H), 7.49 (d, *J* = 8.0 Hz, 1H), 7.45 (t, *J* = 8.0 Hz, 1H), 6.56 (d, *J* = 2.4 Hz, 1H), 6.43 (d, *J* = 2.4 Hz, 1H), 4.05 (t, *J* = 6.4 Hz, 2H), 3.44 (t, *J* = 6.8 Hz, 2H), 1.93-1.87 (m, 2H), 1.86-1.81 (m, 2H), 1.58-1.51 (m, 4H).

4.1.4. General procedure for the synthesis of secondary amines (6a-f)

Compounds **6a-f** were prepared as previously described.[46]

4.1.5. General procedure for the synthesis of 1-hydroxyl-3-aminoalkoxythioxanthen derivatives (7a-f, 8a-f and 9a-f)

Anhydrous potassium carbonate (44.2 mg, 0.32 mmol) and appropriate intermediates **3-5** (0.21 mmol) were added to a solution of the corresponding secondary amines **6a-f** (0.32 mmol) in acetonitrile (2 mL). The reaction mixture was refluxed for 4-9 h. Upon completion of the reaction, the solvent was evaporated under reduced pressure. Water (5 mL) was added to the residue and the mixture was extracted with dichloromethane (5 mL × 4). The combined organic phases were washed with saturated aqueous sodium chloride (20 mL), dried over anhydrous sodium sulfate and then concentrated at reduced pressure. The resultant oil was purified via silica gel chromatography to give compounds **7a-f**, **8a-f** and **9a-f**, respectively.

4.1.5.1. 3-(3-(benzyl(methyl)amino)propoxy)-1-hydroxy-9*H*-thioxanthen-9-one (7a)

It was prepared from 3-(3-bromopropoxy)-1-hydroxy-9*H*-thioxanthen-9-one (**3**) and *N*-benzylmethylamine (**6a**) according to the general procedure, then purified on a silica gel chromatography eluted with petroleum ether/acetone (5:1) to obtain the pure product **7a**. 70.5% yield;

a yellow oil. Purity: 99.1%. ^{1}H NMR (400 MHz, $CDCl_3$) δ 14.44 (s, 1H), 8.54 (d, J = 8.0 Hz, 1H), 7.58 (t, J = 8.0 Hz, 1H), 7.47 (t, J = 8.0 Hz, 1H), 7.43 (d, J = 8.0 Hz, 1H), 7.31−7.24 (m, 5H), 6.50 (s, 1H), 6.40 (s, 1H), 4.02 (t, J = 6.4 Hz, 2H), 3.54 (s, 2H), 2.56 (t, J = 6.8 Hz, 2H), 2.26 (s, 3H), 2.04−1.98 (m, 2H); ^{13}C NMR (100 MHz, $CDCl_3$) δ 184.0, 167.2, 164.1, 140.1, 138.4, 137.1, 132.5, 129.1, 129.0 (2C), 128.4, 128.2 (2C), 127.1, 126.1, 125.3, 109.4, 102.1, 99.9, 66.4, 62.3, 53.2, 42.1, 26.8. HR-ESI-MS: Calcd. for $C_{24}H_{24}NO_3S$ $[M + H]^+$: 406.1477, found: 406.1459.

4.1.5.2. 3-(3-(benzyl(ethyl)amino)propoxy)-1-hydroxy-9*H*-thioxanthen-9-one (7b)

It was prepared from 3-(3-bromopropoxy)-1-hydroxy-9*H*-thioxanthen-9-one (**3**) and *N*-benzylethylamine (**6b**) according to the general procedure, then purified on a silica gel chromatography eluted with petroleum ether/acetone (5:1) to obtain the pure product **7b**. 76.1% yield; a yellow oil. Purity: 98.8%. ^{1}H NMR (400 MHz, $CDCl_3$) δ 14.45 (s, 1H), 8.55 (dd, J = 1.2, 8.0 Hz, 1H), 7.60 (t, J = 8.0 Hz, 1H), 7.49 (t, J = 8.0 Hz, 1H), 7.45 (d, J = 8.0 Hz, 1H), 7.33−7.28 (m, 5H), 6.49 (d, J = 2.4 Hz, 1H), 6.40 (d, J = 2.4 Hz, 1H), 4.07 (t, J = 6.4 Hz, 2H), 3.59 (s, 2H), 2.62−2.53 (m, 4H), 1.97−1.91 (m, 2H), 1.07 (t, J = 7.2 Hz, 3H); ^{13}C NMR (100 MHz, $CDCl_3$) δ 183.9, 167.2, 164.1, 140.0, 139.6, 137.1, 132.4, 129.1, 128.7 (2C), 128.2, 128.1 (2C), 127.1, 126.1, 125.2, 109.4, 102.1, 99.9, 66.5, 58.1, 51.0, 47.4, 26.7, 11.8. HR-ESI-MS: Calcd. for $C_{25}H_{26}NO_3S$ $[M + H]^+$: 420.1633, found: 420.1658.

4.1.5.3. 1-hydroxy-3-(3-((2-methoxybenzyl)(methyl)amino)propoxy)-9*H*-thioxanthen-9-one (7c)

It was prepared from 3-(3-bromopropoxy)-1-hydroxy-9*H*-thioxanthen-9-one (**3**) and *N*-(2-methoxybenzyl)methylamine (**6c**) according to the general procedure, then purified on a silica gel chromatography eluted with dichloromethane/methanol (20:1) to obtain the pure product **7c**. 68.1% yield; a yellow oil. Purity: 98.5%. ^{1}H NMR (400 MHz, $CDCl_3$) δ 14.43 (s, 1H), 8.55 (d, J = 8.0 Hz, 1H), 7.60 (t, J = 8.0 Hz, 1H), 7.49 (d, J = 8.0 Hz, 1H), 7.46 (t, J = 8.0 Hz, 1H), 7.36 (d, J = 7.2 Hz, 1H), 7.26 (t, J = 7.2 Hz, 1H), 6.93 (t, J = 7.2 Hz, 1H), 6.87 (d, J = 7.2 Hz, 1H), 6.54 (d, J = 2.4 Hz, 1H), 6.41 (d, J = 2.4 Hz, 1H), 4.13 (t, J = 6.0 Hz, 2H), 3.89 (s, 3H), 3.71 (s, 2H), 2.76-2.70 (m, 2H), 2.37 (s, 3H), 2.15-2.12 (m, 2H); ^{13}C NMR (150 MHz, $CDCl_3$) δ 184.0, 167.2, 164.0, 157.8, 140.2, 137.1, 132.5, 131.2, 129.1, 129.0, 128.2, 126.1, 125.3, 120.4, 110.5, 110.4, 109.2, 101.9, 100.1, 66.4, 55.4, 55.0, 53.5, 42.0, 26.3. HR-ESI-MS: Calcd. for $C_{25}H_{26}NO_4S$ $[M + H]^+$: 436.1583, found: 436.1595.

4.1.5.4. 3-(3-(ethyl(2-methoxybenzyl)amino)propoxy)-1-hydroxy-9*H*-thioxanthen-9-one (7d)

It was prepared from 3-(3-bromopropoxy)-1-hydroxy-9*H*-thioxanthen-9-one (**3**) and *N*-(2-methoxybenzyl)ethylamine (**6d**) according to the general procedure, then purified on a silica gel chromatography eluted with dichloromethane/methanol (20:1) to obtain the pure product **7d**. 80.6% yield; a yellow oil. Purity: 98.3%. ^{1}H NMR (400 MHz, $CDCl_3$) δ 14.43 (s, 1H), 8.55 (d, J = 8.0 Hz, 1H), 7.60 (t, J = 8.0 Hz, 1H), 7.49 (d, J = 8.0 Hz, 1H), 7.46 (t, J = 8.0 Hz, 1H), 7.39 (d, J = 7.6 Hz, 1H), 7.22 (t, J = 7.6 Hz, 1H), 6.92 (t, J = 7.6 Hz, 1H), 6.85 (d, J = 7.6 Hz, 1H), 6.51 (d, J = 1.6 Hz, 1H), 6.40 (d, J = 1.6 Hz, 1H), 4.09 (t, J = 6.0 Hz, 2H), 3.82 (s, 3H), 3.66 (s, 2H), 2.68-2.61 (m, 4H), 2.04-1.98 (m, 2H), 1.10 (t, J = 6.8 Hz, 3H); ^{13}C NMR (150 MHz, $CDCl_3$) δ 184.0, 167.2, 164.2, 157.7, 140.1, 137.1, 132.4, 130.3, 129.1, 128.2, 128.0, 126.1, 125.3, 120.3, 110.2, 110.0, 109.1, 102.1, 100.0, 66.6, 55.3, 51.4, 49.4, 47.8, 26.7, 11.7. HR-ESI-MS: Calcd. for $C_{26}H_{28}NO_4S$ $[M + H]^+$: 450.1739, found: 450.1723.

4.1.5.5. 3-(3-((2-(dimethylamino)benzyl)(ethyl)amino)propoxy)-1-hydroxy-9*H*-thioxanthen-9-one (7e)

It was prepared from 3-(3-bromopropoxy)-1-hydroxy-9*H*-thioxanthen-9-one (**3**) and 2-((ethylamino)methyl)-*N*,*N*-dimethylaniline (**6e**) according to the general procedure, then purified on a silica gel chromatography eluted with petroleum ether/ethyl acetate (1:2) to obtain the pure product **7e**. 63.6% yield; a yellow oil. Purity: 96.9%. ^{1}H NMR (600 MHz, $CDCl_3$) δ 14.44 (s, 1H), 8.55 (d, J = 7.8 Hz, 1H), 7.60 (t, J = 7.8 Hz, 1H), 7.58-7.54 (m, 1H), 7.50 (d, J = 7.8 Hz, 1H), 7.46 (t, J = 7.8 Hz, 1H), 7.18 (t, J = 7.2 Hz, 1H), 7.08 (d, J = 7.2 Hz, 1H), 7.02 (t, J = 7.2 Hz, 1H), 6.50 (d, J = 2.4 Hz, 1H), 6.40 (d, J = 2.4 Hz, 1H), 4.07 (t, J = 6.6 Hz, 2H), 3.68 (s, 2H), 2.67 (s, 6H), 2.57-2.55 (m, 2H), 1.98-1.94 (m, 2H), 1.68-1.62 (m, 2H), 1.08 (t, J = 6.8 Hz, 3H); ^{13}C NMR (150 MHz, $CDCl_3$) δ 184.0, 167.3, 164.2, 153.0, 140.1, 137.1, 133.7, 132.5, 130.2, 129.1, 128.2, 127.5, 126.2, 125.3, 123.2, 118.9, 109.2, 102.1, 100.0, 66.6, 52.7, 49.5, 47.8, 45.2 (2C), 26.4, 10.1. HR-ESI-MS: Calcd. for $C_{27}H_{31}N_2O_3S$ $[M + H]^+$: 463.2055, found: 463.2097.

4.1.5.6. 3-(3-((4-(dimethylamino)benzyl)(ethyl)amino)propoxy)-1-hydroxy-9*H*-thioxanthen-9-one (7f)

It was prepared from 3-(3-bromopropoxy)-1-hydroxy-9*H*-thioxanthen-9-one (**3**) and 4-((ethylamino)methyl)-*N*,*N*-dimethylaniline (**6f**) according to the general procedure, then purified on a silica gel chromatography eluted with petroleum ether/ethyl acetate (1:2)to obtain the pure product **7f**. 58.1% yield; a yellow oil. Purity: 98.9%. ^{1}H NMR (400 MHz, $CDCl_3$) δ 14.43 (s, 1H),

8.55 (d, *J* = 7.6 Hz, 1H), 7.60 (t, *J* = 7.6 Hz, 1H), 7.49 (d, *J* = 7.6 Hz, 1H), 7.44 (t, *J* = 7.6 Hz, 1H), 7.17 (d, *J* = 8.4 Hz, 2H), 6.55 (d, *J* = 8.4 Hz, 2H), 6.50 (d, *J* = 2.4 Hz, 1H), 6.39 (d, *J* = 2.4 Hz, 1H), 4.05 (t, *J* = 6.4 Hz, 2H), 3.53 (s, 2H), 2.89 (s, 6H), 2.61-2.57 (m, 4H), 1.98-1.94 (m, 2H), 1.09 (t, *J* = 6.4 Hz, 3H); ^{13}C NMR (150 MHz, $CDCl_3$) δ 184.0, 167.2, 164.2, 149.7, 140.0, 137.1, 133.2, 132.4, 129.9, 129.1, 128.2, 126.1, 125.3, 122.0, 120.0, 112.3, 109.1, 102.1, 100.0, 66.5, 57.3, 48.7, 47.3, 40.6 (2C), 26.6, 11.6. HR-ESI-MS: Calcd. for $C_{27}H_{31}N_2O_3S$ $[M + H]^+$: 463.2055, found: 463.2105.

4.1.5.7. 3-(4-(benzyl(methyl)amino)butoxy)-1-hydroxy-9*H*-thioxanthen-9-one (8a)

It was prepared from 3-(4-bromobutoxy)-1-hydroxy-9*H*-thioxanthen-9-one (**4**) and *N*-benzylmethylamine (**6a**) according to the general procedure, then purified on a silica gel chromatography eluted with petroleum ether/acetone (5:1) to obtain the pure product **8a**. 73.9% yield; a yellow oil. Purity: 97.5%. ^{1}H NMR (400 MHz, $CDCl_3$) δ 14.44 (s, 1H), 8.55 (dd, *J* = 1.2, 8.0 Hz, 1H), 7.59 (t, *J* = 8.0 Hz, 1H), 7.48 (d, *J* = 8.0 Hz, 1H), 7.45 (t, *J* = 8.0 Hz, 1H), 7.33−7.25 (m, 5H), 6.54 (d, *J* = 2.0 Hz, 1H), 6.41 (d, *J* = 2.0 Hz, 1H), 4.02 (t, *J* = 6.8 Hz, 2H), 3.53 (s, 2H), 2.45 (t, *J* = 6.8 Hz, 2H), 2.24 (s, 3H), 1.87−1.82 (m, 2H), 1.74−1.69 (m, 2H); ^{13}C NMR (150 MHz, $CDCl_3$) δ 183.9, 167.2, 164.1, 140.1, 138.9, 137.0, 132.4, 129.1, 129.0 (2C), 128.2 (2C), 128.1, 126.9, 126.1, 125.2, 109.1, 102.1, 99.9, 68.2, 62.3, 56.5, 42.1, 26.6, 23.6. HR-ESI-MS: Calcd. for $C_{25}H_{26}NO_3S$ $[M + H]^+$: 420.1633, found: 420.1685.

4.1.5.8. 3-(4-(benzyl(ethyl)amino)butoxy)-1-hydroxy-9*H*-thioxanthen-9-one (8b)

It was prepared from 3-(4-bromobutoxy)-1-hydroxy-9*H*-thioxanthen-9-one (**4**) and *N*-benzylethanamine (**6b**) according to the general procedure, then purified on a silica gel chromatography eluted with petroleum ether/acetone (5:1) to obtain the pure product **8b**. 76.0% yield; a yellow oil. Purity: 97.7%. ^{1}H NMR (400 MHz, $CDCl_3$) δ 14.44 (s, 1H), 8.55 (d, *J* = 7.2 Hz, 1H), 7.59 (t, *J* = 7.2 Hz, 1H), 7.49 (d, *J* = 7.2 Hz, 1H), 7.46 (t, *J* = 7.2 Hz, 1H), 7.36−7.25 (m, 5H), 6.52 (d, *J* = 2.0 Hz, 1H), 6.41 (d, *J* = 2.0 Hz, 1H), 3.98 (t, *J* = 6.4 Hz, 2H), 3.61 (s, 2H), 2.56−2.52 (m, 4H), 1.85−1.79 (m, 2H), 1.68-1.65 (m, 2H), 1.08 (t, *J* = 6.4 Hz, 3H); ^{13}C NMR (150 MHz, $CDCl_3$) δ 183.8, 167.2, 164.0, 140.1, 138.9, 137.0, 132.4, 129.0, 128.9 (2C), 128.1 (2C), 128.0, 126.9, 126.0, 125.2, 109.0, 102.0, 99.9, 68.1, 57.9, 52.3, 47.2, 26.6, 23.2, 11.6. HR-ESI-MS: Calcd. for $C_{26}H_{28}NO_3S$ $[M + H]^+$: 434.1790, found: 434.1763.

4.1.5.9. 1-hydroxy-3-(4-((2-methoxybenzyl)(methyl)amino)butoxy)-9*H*-thioxanthen-9-one (8c)

It was prepared from 3-(4-bromobutoxy)-1-hydroxy-9*H*-thioxanthen-9-one (**4**) and *N*-(2-methoxybenzyl)methylamine (**6c**) according to the general procedure, then purified on a silica gel chromatography eluted with dichloromethane/methanol (15:1) to obtain the pure product **8c**. 80.1% yield; a yellow oil. Purity: 98.3%. ^{1}H NMR (400 MHz, $CDCl_3$) δ 14.44 (s, 1H), 8.55 (dd, J = 0.8, 7.6 Hz, 1H), 7.60 (t, J = 7.6 Hz, 1H), 7.49 (d, J = 7.6 Hz, 1H), 7.46 (t, J = 7.6 Hz, 1H), 7.41 (d, J = 7.2 Hz, 1H), 7.31−7.29 (m, 1H), 6.96 (t, J = 7.2 Hz, 1H), 6.89 (d, J = 7.2 Hz, 1H), 6.54 (d, J = 2.4 Hz, 1H), 6.41 (d, J = 2.4 Hz, 1H), 4.04 (t, J = 6.4 Hz, 2H), 3.83 (s, 3H), 3.74 (s, 2H), 2.66-2.62 (m, 2H), 2.38 (s, 3H), 1.88-1.84 (m, 4H); ^{13}C NMR (150 MHz, $CDCl_3$) δ 183.9, 167.2, 164.0, 157.9, 140.2, 137.0, 132.5, 131.4, 129.3, 129.0, 128.1, 126.1, 125.3, 120.5, 110.5, 110.3, 109.2, 102.0, 99.9, 68.0, 56.3, 55.4, 54.7, 41.5, 26.6, 23.0. HR-ESI-MS: Calcd. for $C_{26}H_{28}NO_4S$ $[M + H]^+$: 450.1739, found: 450.1699.

4.1.5.10. 3-(4-(ethyl(2-methoxybenzyl)amino)butoxy)-1-hydroxy-9*H*-thioxanthen-9-one (8d)

It was prepared from 3-(4-bromobutoxy)-1-hydroxy-9*H*-thioxanthen-9-one (**4**) and *N*-(2-methoxybenzyl)ethanamine (**6d**) according to the general procedure, then purified on a silica gel chromatography eluted with dichloromethane/methanol (15:1) to obtain the pure product **8d**. 73.9% yield; a yellow oil. Purity: 99.0%. ^{1}H NMR (400 MHz, $CDCl_3$) δ 14.43 (s, 1H), 8.55 (d, J = 8.0 Hz, 1H), 7.60 (t, J = 8.0 Hz, 1H), 7.50-7.44 (m, 3H), 7.28-7.24 (m, 1H), 6.96 (t, J = 7.2 Hz, 1H), 6.87 (d, J = 7.2 Hz, 1H), 6.53 (s, 1H), 6.40 (s, 1H), 4.03-3.98 (m, 2H), 3.84 (s, 5H), 2.69-2.66 (m, 4H), 1.84-1.80 (m, 4H), 1.25-1.18 (m, 3H); ^{13}C NMR (150 MHz, $CDCl_3$) δ 183.9, 167.3, 164.0, 157.8, 140.2, 137.1, 132.5, 131.0, 129.1, 128.7, 128.2, 126.2, 125.3, 120.6, 110.4, 110.3, 109.2, 102.0, 99.9, 68.1, 55.4, 52.3, 50.9, 47.5, 26.7, 22.7, 11.0. HR-ESI-MS: Calcd. for $C_{27}H_{30}NO_4S$ $[M + H]^+$: 464.1896, found: 464.1937.

4.1.5.11. 3-(4-((2-(dimethylamino)benzyl)(ethyl)amino)butoxy)-1-hydroxy-9*H*-thioxanthen-9-one (8e)

It was prepared from 3-(4-bromobutoxy)-1-hydroxy-9*H*-thioxanthen-9-one (**4**) and 2-((ethylamino)methyl)-*N*,*N*-dimethylaniline (**6e**) according to the general procedure, then purified on a silica gel chromatography eluted with petroleum ether/ethyl acetate (1:2) to obtain the pure product **8e**. 55.3% yield; a yellow oil. Purity: 95.8%. ^{1}H NMR (600 MHz, $CDCl_3$) δ 14.44 (s, 1H), 8.55 (d, J = 7.8 Hz, 1H), 7.81-7.78 (m, 1H), 7.60 (t, J = 7.8 Hz, 1H), 7.50 (d, J = 7.8 Hz, 1H), 7.47 (t, J = 7.8 Hz, 1H), 7.29-7.20 (m, 1H), 7.16-7.08 (m, 2H), 6.51(d, J = 1.8 Hz, 1H), 6.39 (d, J = 1.8 Hz,

1H), 4.09 (t, *J* = 6.6 Hz, 2H), 2.78 (s, 2H), 2.67 (s, 6H), 2.58-2.54 (m, 4H), 2.06-1.64 (m, 4H), 1.27-1.23 (m, 3H); ^{13}C NMR (150 MHz, $CDCl_3$) δ 183.9, 167.2, 163.9, 153.5, 140.3, 137.1, 132.5, 131.2, 129.1, 129.0, 128.1, 126.2, 125.3, 124.0, 119.6, 115.2, 109.3, 102.0, 99.9, 67.8, 59.5, 51.8, 47.2, 45.0 (2C), 44.9, 26.5, 22.0. HR-ESI-MS: Calcd. for $C_{28}H_{33}N_2O_3S$ $[M + H]^+$: 477.2212, found: 477.2183.

4.1.5.12. 3-(4-((4-(dimethylamino)benzyl)(ethyl)amino)butoxy)-1-hydroxy-9*H*-thioxanthen-9-one (8f)

It was prepared from 3-(4-bromobutoxy)-1-hydroxy-9*H*-thioxanthen-9-one (**4**) and 4-((ethylamino)methyl)-*N*,*N*-dimethylaniline (**6f**) according to the general procedure, then purified on a silica gel chromatography eluted with petroleum ether/ethyl acetate (1:2) to obtain the pure product **8f**. 58.9% yield; a yellow oil. Purity: 98.4%. ^{1}H NMR (600 MHz, $CDCl_3$) δ 14.44 (s, 1H), 8.55 (dd, *J* = 1.2, 7.8 Hz, 1H), 7.61 (t, *J* = 7.8 Hz, 1H), 7.50 (d, *J* = 7.8 Hz, 1H), 7.47 (t, *J* = 7.8 Hz, 1H), 7.28-7.24 (m, 2H), 6.66 (d, *J* = 8.4 Hz, 2H), 6.54 (d, *J* = 2.4 Hz, 1H), 6.40 (d, *J* = 2.4 Hz, 1H), 4.02 (t, *J* = 5.4 Hz, 2H), 3.79 (s, 2H), 2.91 (s, 6H), 2.80-2.71 (m, 4H), 1.85-1.84 (m, 4H), 1.25-1.20 (m, 3H); ^{13}C NMR (150 MHz, $CDCl_3$) δ 183.9, 167.2, 163.8, 150.3, 140.2, 137.0, 132.5, 130.9, 129.0, 128.3, 128.1, 126.1, 125.8, 125.3, 112.4, 112.2, 109.2, 101.9, 99.9, 67.7, 56.4, 51.1, 46.7, 40.3 (2C), 26.4, 21.8, 10.4. HR-ESI-MS: Calcd. for $C_{28}H_{33}N_2O_3S$ $[M + H]^+$: 477.2212, found: 477.2158.

4.1.5.13. 3-((6-(benzyl(methyl)amino)hexyl)oxy)-1-hydroxy-9*H*-thioxanthen-9-one (9a)

It was prepared from 3-((6-bromohexyl)oxy)-1-hydroxy-9*H*-thioxanthen-9-one (**5**) and *N*-benzylmethylamine (**6a**) according to the general procedure, then purified on a silica gel chromatography eluted with petroleum ether/acetone (4:1) to obtain the pure product **9a**. 68.9% yield; a yellow oil. Purity: 98.1%. ^{1}H NMR (400 MHz, $CDCl_3$) δ 14.44 (s, 1H), 8.55 (d, *J* = 8.0 Hz, 1H), 7.59 (t, *J* = 8.0 Hz, 1H), 7.48 (d, *J* = 8.0 Hz, 1H), 7.46 (t, *J* = 8.0 Hz, 1H), 7.34−7.28 (m, 5H), 6.55 (d, *J* = 2.0 Hz, 1H), 6.42 (d, *J* = 2.0 Hz, 1H), 4.02 (t, *J* = 6.4 Hz, 2H), 3.50 (s, 2H), 2.45 (t, *J* = 6.8 Hz, 2H), 2.26 (s, 3H), 1.84−1.77 (m, 2H), 1.65−1.59 (m, 2H), 1.51−1.44 (m, 2H), 1.43−1.39 (m, 2H); ^{13}C NMR (150 MHz, $CDCl_3$) δ 184.0, 167.3, 164.2, 140.1, 137.9, 137.1, 132.4, 129.2 (2C), 129.1, 128.3 (2C), 128.2, 127.2, 126.1, 125.3, 109.1, 102.2, 99.9, 68.4, 62.0, 57.0, 41.9, 28.9, 27.0, 26.8, 25.8. HR-ESI-MS: Calcd. for $C_{27}H_{30}NO_3S$ $[M + H]^+$: 448.1946, found: 448.1905.

4.1.5.14. 3-((6-(benzyl(ethyl)amino)hexyl)oxy)-1-hydroxy-9*H*-thioxanthen-9-one (9b)

It was prepared from 3-((6-bromohexyl)oxy)-1-hydroxy-9*H*-thioxanthen-9-one (**5**) and *N*-benzylethanamine (**6b**) according to the general procedure, then purified on a silica gel chromatography eluted with petroleum ether/acetone (5:1) to obtain the pure product **9b**. 62.5% yield; a yellow oil. Purity: 98.4%. ^{1}H NMR (400 MHz, $CDCl_3$) δ 14.45 (s, 1H), 8.55 (d, J = 8.0 Hz, 1H), 7.60 (t, J = 8.0 Hz, 1H), 7.50 (d, J = 8.0 Hz, 1H), 7.46 (t, J = 8.0 Hz, 1H), 7.39−7.25 (m, 5H), 6.57 (d, J = 2.0 Hz, 1H), 6.44 (d, J = 2.0 Hz, 1H), 4.03 (t, J = 6.4 Hz, 2H), 3.65 (s, 2H), 2.59 (q, J = 6.8 Hz, 2H), 2.51 (t, J = 6.4 Hz, 2H), 1.83−1.77 (m, 2H), 1.57−1.50 (m, 2H), 1.48−1.42 (m, 2H), 1.41−1.37 (m, 2H), 1.10 (t, J = 6.8 Hz, 3H); ^{13}C NMR (100MHz, $CDCl_3$) δ 183.9, 167.3, 164.2, 140.1, 138.5, 137.1, 132.4, 129.2, 129.0 (2C), 128.2 (2C), 128.1, 127.0, 126.1, 125.3, 109.1, 102.1, 99.9, 68.4, 57.8, 52.7, 47.1, 28.9, 27.0, 26.5, 25.7, 11.3. HR-ESI-MS: Calcd. for $C_{28}H_{32}NO_3S$ $[M + H]^+$: 462.2103, found: 462.2163.

4.1.5.15. 1-hydroxy-3-((6-((2-methoxybenzyl)(methyl)amino)hexyl)oxy)-9*H*-thioxanthen-9-one (9c)

It was prepared from 3-((6-bromohexyl)oxy)-1-hydroxy-9*H*-thioxanthen-9-one (**5**) and *N*-(2-methoxybenzyl)methylamine (**6c**) according to the general procedure, then purified on a silica gel chromatography eluted with dichloromethane/methanol (15:1) to obtain the pure product **9c**. 71.1% yield; a yellow oil. Purity: 98.1%. ^{1}H NMR (400 MHz, $CDCl_3$) δ 14.44 (s, 1H), 8.55 (d, J = 8.0 Hz, 1H), 7.59 (t, J = 8.0 Hz, 1H), 7.50−7.44 (m, 3H), 7.32 (t, J = 7.6 Hz, 1H), 6.98 (t, J = 7.6 Hz, 1H), 6.89 (d, J = 7.6 Hz, 1H), 6.56 (d, J = 2.0 Hz, 1H), 6.42 (d, J = 2.0 Hz, 1H), 4.02 (t, J = 6.4 Hz, 2H), 3.88 (s, 2H), 3.85 (s, 3H), 2.72-2.68 (m, 2H), 2.45 (s, 3H), 1.83−1.78 (m, 4H), 1.51−1.47 (m, 2H), 1.45−1.41 (m, 2H); ^{13}C NMR (150 MHz, $CDCl_3$) δ 183.9, 167.2, 164.1, 157.9, 140.2, 137.1, 132.5, 132.0, 129.8, 129.0, 128.1, 126.1, 125.3, 120.7, 110.6, 110.4, 109.1, 102.1, 99.9, 68.2, 56.4, 55.4, 55.3, 54.2, 40.8, 28.7, 26.8, 25.6. HR-ESI-MS: Calcd. for $C_{28}H_{32}NO_4S$ $[M + H]^+$: 478.2052, found: 478.2013.

4.1.5.16. 3-((6-(ethyl(2-methoxybenzyl)amino)hexyl)oxy)-1-hydroxy-9*H*-thioxanthen-9-one (9d)

It was prepared from 3-((6-bromohexyl)oxy)-1-hydroxy-9*H*-thioxanthen-9-one (**5**) and *N*-(2-methoxybenzyl)ethanamine (**6d**) according to the general procedure, then purified on a silica gel chromatography eluted with dichloromethane/methanol (15:1) to obtain the pure product **9d**. 73.8% yield; a yellow oil. Purity: 98.2%. ^{1}H NMR (600 MHz, $CDCl_3$) δ 14.45 (s, 1H), 8.54 (d, J = 7.8 Hz, 1H), 7.59 (t, J = 7.8 Hz, 2H), 7.49 (d, J = 7.8 Hz, 1H), 7.46 (t, J = 7.8 Hz, 1H), 7.32 (t, J =

7.8 Hz, 1H), 7.00 (t, *J* = 7.8 Hz, 1H), 6.89 (d, *J* = 7.8 Hz, 1H), 6.55 (d, *J* = 2.4 Hz, 1H), 6.42 (d, *J* = 2.4 Hz, 1H), 4.05 (t, *J* = 6.6 Hz, 2H), 3.97 (s, 2H), 3.86 (s, 3H), 2.87-2.83 (m, 2H), 2.77-2.73 (m, 2H), 1.82−1.78 (m, 4H), 1.51−1.46 (m, 2H), 1.41−1.36 (m, 2H), 1.28−1.25 (m, 3H); ^{13}C NMR (100 MHz, $CDCl_3$) δ 183.9, 167.2, 164.0, 157.8, 140.2, 137.0, 132.4, 131.9, 129.8, 129.0, 128.1, 126.1, 125.2, 120.8, 110.5, 110.4, 109.1, 102.0, 99.8, 68.1, 55.4, 52.1, 50.4, 47.1, 28.7, 26.8, 25.5, 24.8, 10.1. HR-ESI-MS: Calcd. for $C_{29}H_{34}NO_4S$ $[M + H]^+$: 492.2209, found: 492.2256.

4.1.5.17. 3-((6-((2-(dimethylamino)benzyl)(ethyl)amino)hexyl)oxy)-1-hydroxy-9*H*-thioxanthen-9-one (9e)

It was prepared from 3-((6-bromohexyl)oxy)-1-hydroxy-9*H*-thioxanthen-9-one (**5**) and 2-((ethylamino)methyl)-*N*,*N*-dimethylaniline (**6e**) according to the general procedure, then purified on a silica gel chromatography eluted with petroleum ether/ethyl acetate (1:2) to obtain the pure product **9e**. 49.8% yield; a yellow oil. Purity: 95.6%. ^{1}H NMR (400 MHz, $CDCl_3$) δ 14.44 (s, 1H), 8.55 (dd, *J* = 0.8, 7.6 Hz, 1H), 7.82-7.80 (m, 1H), 7.59 (t, *J* = 7.6 Hz, 1H), 7.48 (d, *J* = 7.6 Hz, 1H), 7.45 (t, *J* = 7.6 Hz, 1H), 7.30-7.27 (m, 1H), 7.16-7.11 (m, 2H), 6.55(d, *J* = 2.0 Hz, 1H), 6.41 (d, *J* = 2.0 Hz, 1H), 4.03 (t, *J* = 6.6 Hz, 2H), 4.00 (s, 2H), 2.83-2.72 (m, 4H), 2.67 (s, 6H), 1.82-1.75 (m, 2H), 1.72-1.69 (m, 2H), 1.50−1.42 (m, 2H), 1.39−1.32 (m, 2H), 1.25−1.22 (m, 3H); ^{13}C NMR (100 MHz, $CDCl_3$) δ 183.9, 167.3, 164.1, 153.3, 140.2, 137.1, 133.8, 132.5, 130.9, 129.1, 128.5, 126.1, 125.3, 123.8, 123.1, 119.4, 109.1, 102.1, 99.9, 68.3, 52.5, 51.6, 47.2, 45.4 (2C), 29.6, 28.8, 26.9, 25.7, 10.5. HR-ESI-MS: Calcd. for $C_{30}H_{37}N_2O_3S$ $[M + H]^+$: 505.2525, found: 505.2517.

4.1.5.18. 3-((6-((4-(dimethylamino)benzyl)(ethyl)amino)hexyl)oxy)-1-hydroxy-9*H*-thioxanthen-9-one (9f)

It was prepared from 3-((6-bromohexyl)oxy)-1-hydroxy-9*H*-thioxanthen-9-one (**5**) and 4-((ethylamino)methyl)-*N*,*N*-dimethylaniline (**6f**) according to the general procedure, then purified on a silica gel chromatography eluted with petroleum ether/ethyl acetate (1:2) to obtain the pure product **9f**. 51.0% yield; a yellow oil. Purity: 98.7%. ^{1}H NMR (400 MHz, $CDCl_3$) δ 14.44 (s, 1H), 8.53 (dd, *J* = 0.8, 7.6 Hz, 1H), 7.59 (t, *J* = 7.6 Hz, 1H), 7.47 (t, *J* = 7.6 Hz, 1H), 7.44 (d, *J* = 7.6 Hz, 1H), 7.27 (d, *J* = 8.8 Hz, 2H), 6.69 (d, *J* = 8.8 Hz, 2H), 6.54 (d, *J* = 2.4 Hz, 1H), 6.41 (d, *J* = 2.4 Hz, 1H), 4.01 (t, *J* = 6.4 Hz, 2H), 3.75 (s, 2H), 2.94 (s, 6H), 2.74 (q, *J* = 6.8 Hz, 2H), 2.62 (t, *J* = 7.2 Hz, 2H), 1.83-1.76 (m, 2H), 1.69-1.67 (m, 2H), 1.51-1.43 (m, 2H), 1.41-1.35 (m, 2H), 1.23 (t, *J* = 6.8 Hz, 3H); ^{13}C NMR (100 MHz, $CDCl_3$) δ 183.9, 167.3, 164.1, 150.2, 140.2, 137.1, 133.8, 132.5, 130.8,

129.1, 128.1, 126.1, 125.3, 123.1, 122.0, 112.3, 109.1, 102.1, 99.9, 68.2, 56.5, 51.7, 46.5, 40.4 (2C), 28.8, 26.8, 25.6, 25.2, 10.4. HR-ESI-MS: Calcd. for $C_{30}H_{37}N_2O_3S$ $[M + H]^+$: 505.2525, found: 505.2503.

4.2. Biological activity

4.2.1. Inhibitory activities of AChE and BuChE

AChE and BuChE inhibitory activities were determined according to the modified Ellman's method[34] using AChE from *Electrophorus electricus* (*Ee*AChE, Sigma-Aldrich Co.) and BuChE from rat serum (*Rat*BuChE). Donepezil was used as a reference compound. For *Ee*AChE inhibition assay, the reaction mixture (100 μL) consisted of acetylthiocholine iodide (ATCI, 1 mM, 30 μL) (J&K Scientific), phosphate buffer solution (0.1 mM, pH = 8.0, 40 μL), different concentrations of test compounds (20 μL) and *Ee*AChE (0.05 U/mL, final concentration, 10 μL). Then 5,5'-dithiobis-2-nitrobenzoic acid (DTNB, 0.2%, 30 μL) (J&K Scientific) was added and the mixture was incubated at 37 °C for 15 min. The absorbance was measured at 412 nm in a Varioskan Flash Multimode Reader (Thermo Scientific). For BuChE inhibition assays, 25% rat serum (10 μL) and S-butylthiocholine iodide (BTCI, 1 mM, 30 μL) (TCI Shanghai Development) were used and the assay was carried out in a phosphate buffer (0.1 mM, pH = 7.4). Changes in absorbance were detected at 405 nm.[34,47] The other procedure was similar with the method described above. IC_{50} values were calculated as the concentration of compound that produces 50% AChE or BuChE activity inhibition. Results are expressed as the mean ± SD of at least three different experiments performed in triplicate.

4.2.1.1. Kinetic study of AChE Inhibition

Kinetic study of AChE inhibition was performed using purified *Ee*AChE based on a reported method.[47] A mixture of phosphate buffer (0.1 M, pH = 8.0), *Ee*AChE (0.5 U/mL), DTNB (0.2%) and different concentrations of tested compounds solution was added and incubated at 37 °C for 15 min. Then substrate in different concentrations was added (0.1-0.4 mM) quickly. Kinetic characterization of the hydrolysis of ATCh catalyzed by *Ee*AChE was done at 412 nm. The parallel control experiments were performed without inhibitor in the assay. The plots were assessed by a weighted least-squares analysis that assumed the variance of velocity (v) to be a constant percentage of v for the entire data set. Slopes of these reciprocal plots were then plotted against the concentration of **9e**

in a weighted analysis and K_i was determined as the intercept on the negative *x*-axis.

4.2.1.2. Molecular Docking of AChE.

Docking studies were performed using AUTODOCK 4.2 program. The crystal structure of AChE (PDB: 1EVE) complexed with donepezil was obtained from the Protein Data Bank after the water molecules and original inhibitors were removed. The 3D Structure of **9e** was built and optimized by molecular mechanics. The inhibitor was prepared furtherly by removing the hydrogen atoms, adding Gasteiger charges and their atomic charges to skeleton atoms, assigning the proper atomic types. Autotors was used to define which bonds were rotatable in ligands. By using Autodock Tools (ADT; version 1.5.6), polar hydrogen atoms were added to amino acid residues and Gasteiger charges were assigned to all atoms of the enzyme. The resulting enzyme structure was used as an input for the AUTOGRID program. AUTOGRID performed a pre-calculated atomic affinity grid maps for each atom type in the ligand, plus an electrostatics map and a separate desolvation map presented in the substrate molecule. All maps were calculated with 0.375 Å spacing between grid points. The center of the grid box was placed at the center of donepezil with coordinates x = 2.023, y = 63.295, z = 67.062. The dimensions of the active site box were set at 60 × 60 × 60 Å. Flexible ligand docking was performed for the compounds. Other than the referred parameters above, the other parameters were used as default. Each docking system was derived from 100 runs of the AUTODOCK using the Lamarckian genetic algorithm (LGA). Finally, a cluster analysis was performed on the docking results using a root mean square (RMS) tolerance of 1.0. Graphic manipulations and visualizations were done by Autodock Tools or Discovery Studio 2.5 software. Took into account the binding energy and the conformational distribution, the most stable binding mode of **9e** to AChE was graphically inspected (binding energy: -12.34 kcal/mol, inhibit constant: 0.904 nM).

4.2.2. Inhibition studies of MAO-A and MAO-B

Recombinant human MAO-A and –B were employed as enzyme sources, and their activities were determined by a fluorimetric method with kynuramine as a common substrate.[48,49] Recombinant human MAO-A and –B were purchased from Sigma-Aldrich and stored at -80 °C. All the enzymatic reactions were performed in potassium phosphate buffer (100 mM, pH = 7.4, containing 20.2 mM KCl) to a final volume of 500 μL containing kynuramine (45 μM for MAO-A and 30 μM for MAO-B) and various concentrations of test compounds (0-100 μM) with the concentration of DMSO lower

than 4%. Solutions of test compounds were dissolved in DMSO in 2.5 mM and diluted using the potassium phosphate buffer (100 mM, pH = 7.4, containing 20.2 mM KCl). By adding MAO-A or MAO-B (7.5 μg/mL), the reactions were started and the solutions were incubated for 30 min at 37 °C. The reactions were finished by the addition of 400 μL NaOH (2 mol/L) and 1000 μL water, then centrifuged for 10 min at 16000 g. The activity was determined on a Varioskan Flash Multimode Reader (Thermo Scientific) by measuring the fluorescence of the supernatant with excitation at 310 nm and emission at 400 nm. IC_{50} values were calculated from sigmoidal dose-response curves (graphs of the initial rate of kynuramine oxidation versus the logarithm of inhibitor concentration). Each sigmoidal curve was constructed from six different compound concentrations spanning at least three orders of magnitude. Data analyses were carried out with GraphPad Prism 5 employing the one site competition model. IC_{50} values were determined in triplicate and expressed as mean ± SD.

4.2.2.1. Molecular modeling study of MAO

Docking studies were performed using AUTODOCK 4.2 program. The X-ray crystal structures of human MAO-A (PDB: 2Z5X) and MAO-B (PDB: 2V60) were obtained from the Protein Data Bank[50]. The original ligands and water molecules were removed and hydrogen atoms were added onto both proteins and cofactors. Each docking system was performed by 100 runs of the Autodock using the Lamarckian genetic algorithm (LGA). The lowest docking-energy conformation of the highest populated cluster was considered as the most stable orientation and could be selected for analysis. Finally, a cluster analysis was performed on the docking results using a root mean square (RMS) tolerance of 1.0. Graphic manipulations and visualizations were done by Autodock Tools or Discovery Studio 2.5 software.

4.2.3. Inhibition of self- and Cu^{2+}-induced Aβ_{1-42} aggregation

To investigate the self-induced Aβ_{1-42} aggregation, a Thioflavin T-based fluorometric assay was performed.[34-35,51] Aβ_{1-42} was purchased from ChinaPeptides Co., Ltd. Thioflavin T (Basic Yellow 1, ThT) was purchased from TCI (Shanghai) Development. Hexafluoro-2-propanol (HFIP) was purchased from Energy Chemical. Aβ_{1-42} was dissolved in HFIP (1 mg/mL) and incubated for 24 h at room temperature. Upon the solvent was evaporated, HFIP pretreated Aβ_{1-42} was dissolved in dry DMSO to obtain a stable stock solution with a concentration of 200 μM, which was stored at -80 °C until use. Solutions of test compounds were prepared in DMSO in 2.5 mM and diluted with phosphate buffer solution (pH = 7.4). A mixture of the Aβ_{1-42} (20 μL, 25 μM) with the tested

compounds (20 μL, 25 μM) was incubated at 37 °C for 24 h. After incubation, 160 μL of 5 μM ThT in 50 mM glycine-NaOH buffer (pH = 8.5) was added. Fluorescence was measured on a Varioskan Flash Multimode Reader (Thermo Scientific) with excitation and emission wavelengths at 446 nm and 490 nm, respectively. The fluorescence intensities were calculated after subtraction of the background activity. The percentage of inhibition was calculated by the expression $(1\text{-}IF_i/IF_c) \times 100$, in which IF_i and IF_c were the fluorescence intensities obtained for A$\beta_{1\text{-}42}$ in the presence and in the absence of inhibitors after subtracting the background fluorescence, respectively. Each measurement was run in triplicate.

For the inhibition of Cu^{2+}-induced A$\beta_{1\text{-}42}$ aggregation,[9,52] the A$\beta_{1\text{-}42}$ stock solution was diluted in HEPES buffer (20 mM, pH = 6.6, 150 mM NaCl) and the solutions of Cu^{2+} (75 μM) were prepared using the same HEPES buffer. The mixture of A$\beta_{1\text{-}42}$ (20 μL, 25 μM) and Cu^{2+} (20 μL, 25 μM) with or without the tested compound (20 μL, 25 μM) was incubated at 37 °C for 24 h. Then, 190 μL of 5 μM ThT in 50 mM glycine-NaOH buffer (pH = 8.5) was added. Each assay was run in triplicate. The detection method was the same as above.

4.2.4. Antioxidant activity assay

The antioxidant activity was determined by the oxygen radical absorbance capacity-fluorescein (ORAC-FL) assay.[41,53] 2,2'-Azobis(amidinopropane) dihydrochloride (AAPH) was purchased from Accela ChemBio Co., Ltd. Fluorescein (FL) and 6-hydroxy-2,5,7,8-tetramethylchromane-2-carboxylic acid (Trolox) were purchased from TCI (Shanghai) Development. All the assays were carried out in 75 mM phosphate buffer (pH = 7.4), and the final reaction mixture was 200 μL. The tested compound (20 μL) and FL (120 μL, 150 nM final concentration) were placed in a black 96-well plate. The mixture was pre-incubated for 15 min at 37 °C and placed in a Varioskan Flash Multimode Reader (Thermo Scientific). AAPH solution (60 μL, 12 mM final concentration) was then added rapidly using an autosampler and the fluorescence was recorded every minute for 90 min with excitation at 485 nm and emission at 535 nm. Trolox was used as a standard (1-8 μM, final concentration). A blank (FL + AAPH) using phosphate buffer instead of antioxidant calibration were carried out in each assay. The samples were measured at 5 μM. All reaction mixtures were prepared in duplicate, and at least three independent assays were performed for each sample. Antioxidant curves (fluorescence vs time) were normalized to the curve of the blank, and the area under the fluorescence decay curve (AUC) was calculated. The net AUC of a sample was obtained by

subtracting the AUC of the blank. Regression equations between net AUC and Trolox concentrations were calculated. ORAC-FL values were expressed as Trolox equivalents by using the standard curve calculated for each assay, where the ORAC-FL value of Trolox was taken as 1.0, indicating the antioxidant potency of the tested compounds.

4.2.5. Metal-chelating studies[34,37]

The metal-chelating studies were performed with a Varioskan Flash Multimode Reader (Thermo Scientific). The UV absorption spectra of compound **9e**, in the absence or presence of $CuCl_2$, $AlCl_3$, $FeSO_4$, and $ZnCl_2$ were recorded with wavelength ranging from 200 to 600 nm after incubating for 30 min at room temperature. The final volume of reaction mixture was 200 μL, and the final concentrations of tested compound and metals were 37.5 μM. Numerical subtraction of the spectra of the metal alone and the compound alone from the spectra of the mixture gave the difference UV-vis spectra due to complex formation. The stoichiometry of the **9e**-Cu^{2+} complex was determined by titrating the methanol solution of tested compound with ascending of $CuCl_2$. The final concentration of tested compound was 37.5 μM, and the final concentration of Cu^{2+} ranged from 3.75 to 150 μM. The UV spectra were recorded and treated by numerical subtraction of $CuCl_2$ and tested compound at corresponding concentrations, plotted versus the mole fraction of tested compound.

4.2.6. MTT assay for cell viability[42,43]

For cell viability assay, SH-SY5Y cells were seeded into 96-well plates at a density of 4×10^4 cells/mL in Dulbecco's modified Eagle's medium (DMEM) supplemented with 10% fetal bovine serum (FBS), and incubated in a humidified atmosphere containing 5% CO_2 at 37 °C. After 24 h, cells were treated with the test compound at three different concentrations (1, 10 and 100 μM) at 37 °C for 24 h. After this incubation, 100 μL/well of MTT (5 mg/mL) at 37 °C was added and incubated for 3 h. Then, 100 μL/well of DMSO was added to dissolve the formazan crystal formed. Optical density (OD) of each well was measured using Varioskan Flash Multimode Reader (Thermo Scientific) with a test wavelength of 590 nm. Results are expressed as percent viability compared to untreated cells for three independent experiments.

4.2.7 *In vitro* blood-brain barrier permeation assay

The BBB permeability of the compounds was evaluated using the parallel artificial membrane permeation assay of the blood-brain barrier (PAMPA-BBB) described by Di et al.[44] Commercial drugs were purchased from Sigma and Alfa Aesar. Porcine brain lipid (PBL) was purchased from

Avanti Polar Lipids. The donor plate (MATRNPS50) and the acceptor plate (PVDF membrane, pore size 0.45 μm, MAIPN4550) were purchased from Millipore. Filter PDVF membrane units (diameter 25 mm, pore size 0.45 μm) from Pall Corporation were used to filter the samples. Due to the free base of test compounds were difficult to dissolve in PBS/EtOH (70:30) system, 5% tartaric acid aqueous solution was used to prepare the stock solution and then diluted with PBS/EtOH (70:30) to a final concentration of 100 μg/mL. The filter membrane was coated with 4 μL PBL in dodecane (20 μg/mL) and the acceptor wells were filled with 200 μL of PBS/EtOH (70:30). And 350 μL of the compound solutions (100 μg/mL) were added to the donor wells. The acceptor filter plate was carefully put on the donor plate to form a sandwich (consisting of the aqueous donor with test compound on the bottom, lipid membrane in the middle and the aqueous acceptor on the top), which was left undisturbed for 18 h at 25 °C. After incubation, the donor and acceptor plates were separated and the concentration of drug in the donor and acceptor wells was determined using the Varioskan Flash Multimode Reader (Thermo Scientific). Every sample was analyzed at ten wavelengths in four wells and in at least three independent runs. P_e was calculated using the following expression:

$$P_e = -\ln [1 - C_A(t)/C_{equilibrium}]/[A \times (1/V_D + 1/V_A) \times t]$$

$$C_{equilibrium} = [C_D(t) \times V_D + C_A(t) \times V_A]/(V_D + V_A)$$

Where P_e is permeability in the unit of cm/s. A is effective filter area and t is the permeation time. V_D is the volume of donor well and V_A is the volume of acceptor well. $C_A(t)$ is the compound concentration in acceptor well at time t, and $C_D(t)$ is the compound concentration in donor well at time t. Results are given as the mean ± SD. In the experiment, 11 quality control drugs of known BBB permeability were included to validate the analysis set. A plot of the experimental data versus literature values gave a strong linear correlation, P_e (exp.) = 0.8792 × P_e (bibl.) − 0.0616 (R^2 = 0.9555). From this equation and taking into account the limit established by Di et al.[44] for BBB permeation, we determined that compounds with P_e values above 3.46 × 10^{-6} cm/s could cross the BBB.

Acknowledgements

This work was supported in part by the Chinese National Natural Science Foundation (20872099), the Research Fund for the Doctoral Program of Higher Education (20110181110079) and the National Science and Technology Major Project on "Key New Drug Creation and

Manufacturing Program"(2013ZX09301304-002).

Supplementary data

Supplementary data associated with this article can be found, in the online version,

References and notes

1. Piazzi, L.; Rampa, A.; Bisi, A.; Gobbi, S.; Belluti, F.; Cavalli, A.; Bartolini, M.; Andrisano, V.; Valenti, P.; Recanatini, M. *J. Med. Chem.* **2003**, *46*, 2279.
2. Scarpini, E.; Scheltens, P.; Feldman, H. *Lancet Neurol*. **2003**, *2*, 539.
3. Castro, A.; Conde, S.; Rodriguez-Franco, M. I.; Martinez, A. *Mini. Rev. Med. Chem.* **2002**, *2*, 37.
4. Greig, N. H.; Utsuki, T.; Yu, Q. S.; Zhu, X. X.; Holloway, H. W.; Perry, T.; Lee, B.; Ingram, D. K.; Lahiri, D. K. *Curr. Med. Res. Opin.* **2001**, *17*, 159.
5. Querfurth, H. W.; LaFerla, F. M. *N. Engl. J. Med.* **2010**, *362*, 329.
6. Rizzo, S.; Rivière, C.; Piazzi, L.; Bisi, A.; Gobbi, S.; Bartolini, M.; Andrisano, V.; Morroni, F.; Tarozzi, A.; Monti, J. P.; Rampa, A. *J. Med. Chem.* **2008**, *51*, 2883.
7. Reyes, A. E.; Chacón, M. A.; Dinamarca, M. C.; Cerpa, W.; Morgan, C.; Inestrosa, N. C. *Am. J. Pathol.* **2004**, *164*, 2163.
8. Fernández-Bachiller, M. I.; Pérez, C.; Monjas, L.; Rademann, J.; Rodríguez-Franco, M. I. *J. Med. Chem*. **2012**, *55*, 1303.
9. Huang, L.; Lu, C. J.; Sun, Y.; Mao, F.; Luo, Z. H.; Su, T.; Jiang, H. L.; Shan, W. J.; Li, X. S. *J. Med. Chem*. **2012**, *55*, 8483.
10. Paul, S.; Planque, S.; Nishiyama, Y. *Rejuvenation Res.* **2010**, *13*, 179.
11. Edmondson, D. E.; Binda, C.; Wang, J.; Upadhyay, A. K.; Mattevi, A.; *Biochem.* **2009**, *48*, 4220.
12. Patil, P. O.; Bari, S. B.; Firke, S. D.; Deshmukh, P. K.; Donda, S. T.; Patil, D. A. *Bioorg. Med. Chem.* **2013**, *21*, 2434.
13. Maynard, C. J.; Bush, A. I.; Masters, C. L.; Cappai, R.; Li, Q. X. *Int. J. Exp. Pathol.* **2005**, *86*, 147.
14. Reddy, V. P.; Zhu, X. W.; Perry, G.; Smith, M. A. *J. Alzheimer's Dis*. **2009**, *16*, 763.
15. Nunomura, A.; Castellani, R. J.; Zhu, X. W.; Moreira, P. I.; Perry, G.; Smith, M. A. *J. Neuropathol Exp. Neurol.* **2006**, *65*, 631.

16. Huang, M.; Xie, S. S.; Jiang, N.; Lan, J. S.; Kong, L. Y.; Wang, X. B. *Bioorg. Med. Chem. Lett.* **2015**, *25*, 508.

17. Zheng, H. L.; Youdim, M. B. H.; Fridkin, M. *J. Med. Chem.* **2009**, *52*, 4095.

18. Bush, A. I. *J. Alzheimer's Dis*. **2008**, *15*, 223.

19. Zhang, C.; Du, Q. Y.; Chen, L. D.; Wu, W. H.; Liao, S. Y.; Yu, L. H.; Liang, X. T. *Eur. J. Med. Chem.* **2016**, *116*, 200.

20. Cavalli, A.; Bolognesi, M. L.; Minarini, A.; Rosini, M.; Tumiatti, V.; Recanatini, M.; Melchiorre, C. *J. Med. Chem.* **2008**, *51*, 347.

21. León, R.; Garcia, A. G.; Marco-Contelles, J. *Med. Res. Rev*. **2013**, *33*, 139.

22. Agis-Torres, A.; Solhuber, M.; Fernandez, M.; Sanchez-Montero, J. M. *Curr. Neuropharmacol*. **2014**, *12*, 2.

23. Qin, J. K.; Lan, W. L.; Liu, Z.; Huang, J.; Tang, H.; Wang, H. S. *Chem. Cent. J*. **2013**, *7*, 78.

24. Piazzi, L.; Belluti, F.; Bisi, A.; Gobbi, S.; Rizzo, S.; Bartolini, M.; Andrisano, V.; Recanatini, M.; Rampa, A. *Bioorg. Med. Chem*. **2007**, *15*, 575.

25. Wang, S. N.; Li, Q.; Jing, M. H.; Alba, E.; Yang, X. H.; Sabaté, R. Han, Y. F.; Pi, R. B.; Lan, W. J.; Yang, X. B. *Neurochem. Res.* **2016**, *41*, 1806.

26. Foster, B. J.; Wiegand, R. A.; Pugh, S.; Lorusso, P. M.; Rake, J.; Corbett, T. H. *Clin. Cancer Res*. **1997**, *3*, 2047.

27. Bessa, L. J.; Palmeira, A.; Gomes, A. S.; Vasconcelos, V.; Sousa, E.; Pinto, M. *Microb. Drug Resist*. **2015**, *21*, 404.

28. Harfenist, M.; Heuser, D. J.; Joyner, C. T.; Batchelor, J. F.; White, H. L. *J. Med. Chem*. **1996**, *39*, 1857.

29. Qiang, X. M.; Sang, Z. P.; Yuan, W.; Li, Y.; Liu, Q.; Bai, P.; Shi, Y. K.; Tan, Z. H.; Deng, Y. *Eur. J. Med. Chem*. **2014**, *76*, 314.

30. Allen, C. F. H.; MacKay, D. D. *Org. Synth*. **1943**, *2*, 580.

31. Kostakis, I. K.; Pouli, N.; Marakos, P.; Mikros, E.; Leonce, S.; Atassi, G.; Renard, P. *Bioorg. Med. Chem.* **2001**, *9*, 2793.

32. Das, A.; Shaikh, M. M.; Jana, S. *Med. Chem. Res*. **2014**, *23*, 436.

33. Sang, Z. P.; Qiang, X. M.; Li, Y.; Yuan, W.; Liu, Q.; Shi, Y. K.; Ang, W.; Luo, Y. F.; Tan, Z. H.; Deng, Y. *Eur. J. Med. Chem.* **2015**, *94*, 348.

34. Li, Y.; Qiang, X. M.; Luo, L.; Li, Y. X.; Xiao, G. Y.; Tan, Z. H.; Deng, Y. *Bioorg. Med. Chem.* **2016**, *24*, 2342.

35. Rosini, M.; Simoni, E.; Bartolini, M.; Cavalli, A.; Ceccarini, L.; Pascu, N.; Tarozzi, A.; Bolognesi M. L.; Minarini, A. *J. Med. Chem.* **2008**, *51*, 4381.

36. Meena, P.; Nemaysh, V.; Khatri, M.; Manral, A.; Luthra, P. M.; Tiwari, M. *Bioorg. Med. Chem.* **2015**, *23*, 1135.

37. He, Y.; Yao, P. F.; Chen, S. B.; Huang, Z. H.; Huang, S. L.; Tan, J. H.; Li, D.; Gu, L. Q.; Huang, Z. S. *Eur. J. Med. Chem.* **2013**, *63*, 299.

38. Najafi, Z.; Mahdavi, M.; Saeedi, M.; Karimpour-Razkenari, E.; Asatouri, R.; Vafadarnejad, F.; Moghadam, F. H.; Khanavi, M.; Sharifzadeh, M.; Akbarzadeh, T. *Eur. J. Med. Chem.* **2017**, *125*, 1200.

39. Bartolini, M.; Bertucci, C.; Bolognesi, M. L.; Cavalli, A.; Melchiorre, C.; Andrisano, V. *Chembiochem.* **2007**, *8*, 2152.

40. Yang, F. S.; Lim, G. P.; Begum, A. N.; Ubeda, O. J.; Simmons, M. R.; Ambegaokar, S. S.; Chen, P. P.; Kayed, R.; Glabe, C. G.; Frautschy, S. A. *J. Biol. Chem.* **2005**, *280*, 5892.

41. Dávalos, A.; Gómez-Cordovés, C.; Bartolomé, B. *J. Agric. Food Chem.* **2004**, *52*, 48.

42. Fernández-Bachiller, M. I.; Pérez, C.; Campillo, N. E.; Páez, J. A.; González-Muñoz, G. C.; Usán, P.; García-Palomero, E.; López, M. G.; Villarroya, M.; García, A. G.; Martínez, A.; Rodríguez-Franco, M. I. *ChemMedChem*. **2009**, *4*, 828.

43. Xie, S. S.; Lan, J. S.; Wang, X. B.; Wang, Z. M.; Jiang, N.; Li, F.; Wu, J. J.; Wang, J.; Kong, L. Y. *Bioorg. Med. Chem.* **2016**, *24*, 1528.

44. Di, L.; Kerns, E. H.; Fan, K.; Mcconnell, O. J.; Carter, G. T. *Eur. J. Med. Chem.* **2003**, *38*, 223.

45. Sang, Z. P.; Li, Y.; Qiang, X. M.; Xiao, G. Y.; Liu, Q.; Tan, Z. H.; Deng, Y. *Bioorg. Med. Chem.* **2015**, *23*, 668.

46. Kumpaty, H. J.; Williamson, J. S.; Bhattacharyya, S. *Synth. Commun.* **2003**, *33*, 1411.

47. Lu, C. J.; Zhou, Q.; Yan, J.; Du, Z. Y.; Huang, L.; Li, X. S. *Eur. J. Med. Chem.* **2013**, *62*, 745.

48. Li, Y.; Qiang, X. M.; Luo, L.; Yang, X.; Xiao, G. Y.; Liu, Q.; Ai, J. C.; Tan, Z. H.; Deng Y. *Eur. J Med. Chem.* **2017**, 126, 762.

49. Li, Y.; Qiang, X. M.; Luo, L.; Yang, X.; Xiao, G. Y.; Zheng, Y. X. Z.; Cao, Z. C.; Sang, Z. P.; Su, F.; Deng, Y. *Bioorg. Med. Chem.* **2017**, 25, 714.

50. Desideri, N.; Bolasco, A.; Fioravanti, R.; Monaco, L. P.; Orallo, F.; Yáñez, M.; Ortuso, F.; Alcaro, S. *J. Med. Chem.* **2011**, *54*, 2155.

51. Li, R. S.; Wang, X. B.; Hu, X. J.; Kong, L. Y. *Bioorg. Med. Chem. Lett.* **2013**, *23*, 2636.

52. Geng, J.; Li, M.; Wu, L.; Ren, J. S.; Qu, X. G. *J. Med. Chem.* **2012**, *55*, 9146.

53. Fang, L.; Kraus, B.; Lehmann, J.; Heilmann, J.; Zhang, Y. H.; Decker, M. *Bioorg. Med. Chem. Lett.* **2008**, *18*, 2905.

Graphical Abstract

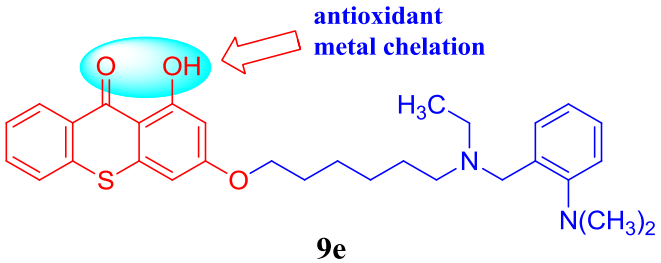

9e

*Ee*AChE IC_{50}: 0.59 ± 0.02 μM; ORAC-FL value: 0.74 ± 0.02 (Trolox equiv)

MAO-A IC_{50}: 1.01 ± 0.02 μM; MAO-B IC_{50}: 0.90 ± 0.01 μM

Self -induced A$\beta_{1\text{-}42}$ aggregation: 74.8 ± 1.2% inhibition at 25 μM

Cu^{2+}-induced A$\beta_{1\text{-}42}$ aggregation: 87.7 ± 1.9% inhibition at 25 μM

Low toxicity in SH-SY5Y cells and could penetrate the BBB